HYDROGEOCHEMISTRY OF TWO CONTRASTING ATOLL ISLAND AQUIFERS, ROI-NAMUR, REPUBLIC OF THE MARSHALL ISLANDS

A Thesis submitted to the faculty of
San Francisco State University
In partial fulfillment of
the requirements for
the Degree

AS
36
2016
GEOL
.H45

Master of Science

In

Geosciences

by

Mehrdad Hejazian

San Francisco, California

May 2016

Copyright by
Mehrdad Hejazian
2016

CERTIFICATION OF APPROVAL

I certify that I have read Hydrogeochemistry of Two Contrasting Atoll Island Aquifers, Roi-Namur, Republic of the Marshall Islands by Mehrdad Hejazian, and that in my opinion this work meets the criteria for approving a thesis submitted in partial fulfillment of the requirement for the degree Master of Science in Geosciences at San Francisco State University.

Jason J. Gurdak, Ph.D.
Associate Professor of Hydrogeology

Mary Leech, Ph.D.
Associate Professor of Geology

for Peter Swarzenski

Peter W. Swarzenski, Ph.D.
International Atomic Energy Agency

HYDROGEOCHEMISTRY OF TWO CONTRASTING ATOLL ISLAND AQUIFERS, ROI-NAMUR, REPUBLIC OF THE MARSHALL ISLANDS

Mehrdad Hejazian
San Francisco, California
2016

Groundwater resources on low-lying atoll islands are extremely vulnerable to climate change and sea-level rise because they are typically <3 m above mean sea level and are composed of relatively permeable rock that drains vital groundwater resources. Because thick, topical vegetation covers large amounts of the landscape, evapotranspiration is high and recharge to aquifers is limited. Since atoll islands are isolated from any mainland, rainwater catchment is their primary source of water supply, but they also rely heavily on groundwater resources, especially during times of drought. Land-use/land-cover (LULC) change and managed aquifer recharge (MAR) have shown promise in increasing groundwater supply on Roi-Namur Island, Republic of the Marshall Islands. Roi-Namur has two lobes, each with contrasting island settings and aquifers. Roi is estimated to have 8.6 x 10^5 m^3 of potable groundwater in the freshwater lens (FWL), compared to only 1.6 x 10^4 m^3 on Namur. This is mostly attributed to the removal of vegetation and MAR on Roi, which was implemented as result of a U.S. military installation on the island. A suite of monitoring wells were sampled on Roi and Namur and a Wilcoxon-rank sum test indicates statistically significant water quality differences between the contrasting aquifers. Results indicate dissolution of carbonate rock in the freshwater lens and overlying vadose zone of Roi has been reduced seven-fold as a result of LULC and MAR. Geochemical modeling with PHREEQC is used to investigate differences in geochemical processes. The more dominant geochemical process on Roi is mixing with seawater due to flushing of the aquifer. In contrast, equilibrium processes and dissolution-precipitation non-equilibrium reactions are more dominant on Namur, at least in part due to longer residence times relative to the rate of geochemical reactions. Results suggest LULC and MAR has successfully increased groundwater supply on Roi-Namur; these methods should be considered as a viable adaptation measure to climate change stressors on inhabited atoll islands.

I certify that the Abstract is a correct representation of the content of this thesis.

Chair, Thesis Committee

5-24-2016
Date

ACKNOWLEDGEMENTS

Foremost, I would like to express my sincere gratitude to my advisor, Professor Jason J. Gurdak, for accepting me into his hydrogeology program and his continuous support of my MS studies and research, and for his patience, expertise, and mentorship throughout my time at SF State University. My graduate studies experience was tremendous and I could not have imagined having a better advisor and mentor. My sincerest appreciation to Dr. Peter W. Swarzenski for giving me the opportunity to do research in one of the most unique places on Earth and allowing me to utilize the resources of the U.S. Geological Survey to accomplish my research. I am forever grateful for his support in completing my MS research. I would like to thank Dr. Kingsley Odigie for his mentorship and assistance in the field; this research would not have been achievable without his incredible support and unwavering patience and fortitude while surrounded by thirsty mosquitoes for many long days in the field. Many thanks to Professor Mary Leech for not only being a member of my thesis committee, but also helping me to realize my passion for geology when I enrolled in her Mineralogy/Petrology class in my first semester at SF State University. I must also thank the many professors along the way that have worked so hard in not only giving me an excellent education but guiding me through an amazing graduate academic experience. This research could not have been accomplished without funding from the U.S. Geologic Survey (USGS), the Department of Defense SERDP project, the Research Institute for Humanity and Nature (RIHN), and the California State University (CSU) Council on Ocean Affairs, Science, and Technology (COAST).

To my dearest mother, Shahla, who has always advocated for my higher education and given me untiring love and support throughout my life, you are my rock and I dedicate this thesis to you. I owe this accomplishment to my father, Akbar, who has worked very hard and sacrificed so much since I was born to give me this opportunity. My brother, Milad, has been a great friend through this experience and someone I could always rely on to be there for me and I truly appreciate his support. I am grateful for the wonderful friends I made at SF State University and the amazing experiences we had together that will always be remembered through our exceptional bond.

TABLE OF CONTENTS

LIST OF TABLES .... *vii*

LIST OF FIGURES .... *viii*

LIST OF APPENDICES .... *ix*

1. Introduction *1*

1.1. Atoll Water Resources 1

1.2 Field Site Description 4

2.0 Background *5*

2.1. Atoll Hydrogeology 5

2.2. Atoll Geochemistry 8

3.0 Methods *9*

3.1. Field Methods and Groundwater Sampling 9

3.2. Laboratory Methods 10

3.3 Water Quality Comparison 10

3.4. Geochemical Modeling 14

4.0 Results *18*

4.1. Freshwater Lens Asymmetry 18

4.2. Water Quality Comparison 21

4.3. Carbonate Dissolution 23

4.4. Equilibrium/Non-equilibrium Reactions 24

5.0 Summary *27*

6.0 Conclusion *29*

7.0 Tables *30*

8.0 Figures *34*

References *46*

Appendix A *49*

Appendix B *51*

Appendix C *52*

LIST OF TABLES

Table Page

1. Groundwater Field Parameters and Concentrations....................................30
2. Results of Wilcoxon Rank-Sum Test......... 32
3. Dissolution Rate and Source Rock Contribution Calculations...........................33

LIST OF FIGURES

Figures Page

1. Field Location Map and Google Earth Image of Roi-Namur 34
2. Dual Aquifer Conceptual Model of Typical Atoll Island 36
3. Salinity Profiles for Roi and Namur 37
4. Groundwater Level Map for Roi-Namur 38
5. Distribution of Residuals for Statistically Different Parameters 39
6. Anthropogenic Effects on Roi Groundwater 40
7. Plot of Saturation Index versus Percent Seawater 41
8. Plot of Log pCO_2 versus Percent Seawater 42
9. DIC Profiles for Roi-Namur 43
10. Theoretical Mixing Scenarios for Roi and Namur 44
11. Saturation Index with Respect to Aragonite as a function of pCO_2 45

LIST OF APPENDICES

Appendix Page

1. Appendix A 49
2. Appendix B...51
3. Appendix C 52

1. Introduction

1.1. Atoll Water Resources

Low-lying atolls are generally <3 m above mean sea level and are particularly vulnerable to climate stressors and sea-level rise (SLR) (Dickinson, 2009). The estimated SLR by the end of the 21st century ranges from 0.26–0.82 m based on the 2014 IPCC report (Pachauri et al., 2014) to 0.6–1.6 m from studies that account for more thermal expansion and additional melt from Greenland and Antarctic Ice Sheets (Jevrejeva et al., 2010). SLR poses a serious threat to communities on atoll islands, and thus many of the >400 atolls worldwide may be uninhabitable by the end of the 21st century (Bailey et al., 2013).

In addition to the SLR-induced inundation of atolls, climatic and population pressures are threatening the sustainability of the freshwater resources on most atoll islands (Karnauskas et al., 2016). In some cases, the lack of freshwater, including groundwater resources, may be a limiting factor for habitability of atolls even before loss of land due to SLR-induced inundation (Gurdak et al., 2015). In addition to SLR, incremental seawater encroachment, more frequent storm over-wash events, and droughts related to El Niño/Southern Oscillation (ENSO) variability over the coming years and decades will reduce land cover and threaten groundwater supplies, forcing inhabitants to adapt or relocate (White et al., 2007). Because groundwater is an important source of freshwater supply on low lying atolls, especially during droughts, any adaptation measures to SLR and climate stressors must include a suitable groundwater management plan.

Freshwater in atoll aquifers floats on top of saline water and is roughly lenticular in shape and is typically referred to as the ‘freshwater lens’ (FWL). The FWL is defined as water with a chloride concentration <250 mg/L, or approximately <1.3% seawater, based on U.S. EPA drinking water standards. Groundwater management plans for atoll islands usually call to increase the resilience of the FWL by focusing on minimizing or eliminating pollution and over-pumping. However, the resilience of the FWL and groundwater supply can also be increased if measures are implemented that favor recharge over evapotranspiration (ET). Tree cover, vegetation, and rainfall variability can have a substantial effect on ET and subsequent recharge to the FWL. For example, empirical relationships show that the percent recharged on some atolls generally increases with increasing mean annual precipitation. Based on methods used by Falkland (1991), a study on Enewetak Atoll found that an atoll island with average annual rainfall of 1040 mm and 0%, 40%, or 80% tree cover equates to 18%, 11%, or 4% recharge, respectively (Buddemeier and Oberdorfer, 1997). In comparison, an annual rainfall of 1878 mm and similar percentages of land with tree cover, recharge increases to 46%, 27%, or 25%, respectively.

In addition to changing the vegetative cover, increasing the groundwater supply can also be accomplished by artificial recharge using a managed aquifer recharge (MAR) system. MAR usually entails collecting surface water during wet periods and taking advantage of seasonal over-supply to replenish an aquifer. In recent years, the use of MAR has greatly increased, particularly in coastal aquifers to minimize seawater intrusion (Vandenbohede et al., 2009). However, the use of MAR on atolls or similarly small islands is not widely reported. One exception is Roi-Namur, a small atoll island leased to the U.S. by the Republic of the Marshall Islands, which has implemented an MAR system and removed most of the native vegetation for a military base. As a result, the groundwater supply has increased significantly for the U.S. military contractors and personnel and local Marshallese who commute to the island as employees of the U.S. Army. However, it is unknown how these changes to the hydrologic system have altered natural geochemical reactions and the quality of groundwater.

Previous studies have characterized the groundwater geochemistry of inhabited atoll and carbonate islands across a range of landscape alteration, rainfall and recharge rates, and sizes and locations (Anthony et al., 1989; Buddemeier and Oberdorfer, 1986; Plummer et al., 1976; Tribble, 1997). However, no study to date has systematically evaluated the link between land-use/land-cover (LULC) change and artificially increasing recharge and the combined effects on groundwater geochemistry. Roi-Namur Island presents a unique setting because a managed aquifer (with altered vegetation and MAR) on Roi, the western lobe of the island, is co-located and directly adjacent to a more naturally recharged aquifer (with natural vegetation and no MAR) on Namur, the eastern lobe (Fig. 1). The aquifer on Roi is estimated to have 8.6 x 10^5 m^3 of (potable) freshwater compared to 1.6 x 10^4 m^3 on Namur (Gingerich, 1996). The 98% difference in total estimated volume of freshwater between Roi and Namur has largely been attributed to differences in ET as a result of less vegetation on Roi (Gingerich, 1996). The same geographic location and relatively similar sizes of these contrasting island hydrologic systems allows for an ideal comparative study of how LULC change and groundwater resource adaptation measures, such as MAR, influence geochemical processes and groundwater supply on atoll islands.

Comparison of the two contrasting aquifers was done by sampling a suite of geochemical parameters from groundwater monitoring wells across the two lobes of the island. The objective was to answer three main questions: Does altered LULC and MAR practices result in statistically significant differences in groundwater quality on the two lobes of the island? Do changes in the recharge quantity and quality caused by the altered LULC and MAR practices affect the aqueous and solid carbonate system with respect to dissolution rates and natural geochemical processes? Is the practice of clearing native vegetation and MAR a suitable adaptation and groundwater sustainability measure for future climate stressors? A better understanding of how LULC change and MAR affect geochemical process and groundwater supply will help provide a framework for best water supply management practices on low-lying and carbonate islands in the context of climate change.

1.2 Field Site Description

Kwajalein Atoll, Republic of the Marshall Islands, is located in the western Pacific at approximately latitude 9°N and longitude 167°E (Fig. 1). It covers an area of 2,850 km^2 and contains the world's largest enclosed lagoon. The subaerial ring-shaped coral reef that surrounds the lagoon has a total land area of 16.4 km^2. Roi-Namur is positioned at the northern-most point of the atoll and is made up of two reef islets (Roi and Namur), which were artificially conjoined by dredge fill during Japanese occupation prior to World War II. Currently, the island is leased to the U.S. military for use as a missile defense site.

Both Roi and Namur house some of the military infrastructure; however, Roi has been mostly cleared of vegetation to accommodate a 1,370-m-long runway, 9-hole golf course, and living quarters for military and civilian personnel. Only thin grasses and relatively few coconut palms remain for aesthetics. Water supply on Roi-Namur is limited to surface catchment and storage during the rainy season and pumping of the FWL during the dry season and at times of drought. Two concrete-lined rainwater catchment basins on Roi are used to collect rainwater that is subsequently pumped into two 2,840 m^3 storage tanks (C.J. Golby-Saunders, 2015, pers. commun.). When the tanks reach capacity, the rainwater is pumped to the western side of the runway and poured over a grassy field to recharge the aquifer. At times of drought and low surface-water supply, groundwater is pumped from the FWL using a 1000-m-long horizontal lens well that parallels the western side of the runway. There are several pumps spaced across the horizontal lens well that skim water from the top of the water table. This type of well pumping system prevents upconing of deeper, saline waters during groundwater withdrawal.

Adjacent to Roi on the windward reef, Namur contains heavy vegetative cover, including coconut palm trees, banana trees, pandanus, and other thick jungle-like scrub vegetation that has been minimally altered (Gingerich, 1992). A few buildings are located on the northern and central part of this lobe, but the difference in LULC between the lobes is substantial. The groundwater on Namur is naturally recharged, but the volume of the FWL is limited by higher ET rates compared to Roi. Because of this, the freshwater lens dynamics are more indicative of natural atoll island settings where human impact has been minimal, yet a thin, viable freshwater lens still exists. A horizontal lens well is located on Namur, but it is not being actively pumped for water supply. In this study we identify Roi as the human-modified lobe and Namur as the natural, vegetated lobe.

2.0 Background

2.1. Atoll Hydrogeology

Atolls are circular or ring-shaped chains of small, coral islands surrounding a shallow lagoon, with a unique hydrogeologic structure and limited freshwater supply (Bailey et al., 2013). Observations of atoll island geology have identified two distinct stratigraphic layers that are controls on the depth of the FWL and tidal efficiency (Ayers and Vacher, 1986; Hunt and Peterson, 1980) (Fig. 2). The bottom layer is a highly permeable Pleistocene limestone layer that overlies basaltic basement rock and can be as thick as 3,000 m in some places (Raitt and Perkins, 1954). The high permeability is due to subaerial diagenesis and the karstification of limestone during low sea-level stands. The upper layer is significantly less permeable and consists of unconsolidated fine-grained Holocene carbonate deposits that are typically <30 m thick, with larger, leeward islands accumulating the thickest deposits. An unconformity delineates the Holocene and Pleistocene stratigraphic layers. Studies such as the ones on Enewetak Atoll (Wardlaw and Quinn, 1991) and Deke Atoll (Ayers and Vacher, 1986) used drilling cores and seismic interpretation to identify this dissolution unconformity, termed the "Thurber Discontinuity", which represents a hiatus in carbonate deposition and subsequent diagenesis between approximately 125 ka and 8 ka during low glacio-eustatic sea-levels (Thurber et al., 1965). Roi-Namur drilling records indicate that consolidated limestone, presumed to be the lower Pleistocene Karst, is located between 7 and 14 m below land surface (bls) (Gingerich, 1992). The depth of the Thurber Discontinuity and bottom layer is consistent with observations from nearby atolls of Enewetak, Bikini, Majuro, and others (Anthony et al., 1989; Buddemeier and Oberdorfer, 1997; Emery et al., 1954). Using the groundwater model SUTRA (Voss, 1984), studies have estimated the hydraulic conductivity (K) of the Holocene sediments to be 10–50 m day^{-1} (Underwood et al., 1992) and for the Pleistocene aquifer a K value of 1,000 m day^{-1} (Oberdorfer et al., 1990).

Freshwater is less dense than saltwater and thus, floats on saltwater in the aquifer, and mixing occurs at the freshwater-saltwater interface. Early observations of coastal groundwater by Ghyben (1888) and Herzberg (1901) indicated that the depth of the freshwater-saltwater interface is linearly proportional to the elevation of the water table above sea level. The Ghyben-Herzberg depth (GHD) is defined by the equation:

$$z = \frac{\rho_f}{\rho_s - \rho_f} h \qquad \text{(eqn. 1)}$$

where ρ_f [M L^{-3}] is the density of freshwater and ρ_s [M L^{-3}] is the density of saltwater, and h [L] and z [L] are the thickness of the freshwater zone above and below sea level, respectively. Equation 1 can be simplified to $z = 40h$, which states that for every unit of freshwater head above sea level in an unconfined aquifer there are forty units below sea level. However, the Ghyben-Herzberg relation is imprecise and overestimates FWL thickness on atoll islands because of their relatively small size, and porous lithology that allows for greater tidal mixing. Observations have identified a thick saline transition zone (sometimes thicker than the FWL) caused by dispersive tidal mixing, which forms a vertical salinity gradient delineating the saltwater-freshwater interface. On larger islands, the thickness of the FWL is limited by the depth of the more permeable Pleistocene layer because these indurated rocks have K values one to two orders of magnitude higher than the upper layer and thus promote greater tidal mixing and truncate the base of the mixing zone (Anthony et al., 1989).

In general, the thickness of the FWL can be seen as a function of average annual rainfall, K of the unconsolidated Holocene deposits, island width, depth to the Thurber Discontinuity, and in some cases the reef flat plate, a relatively thin and shallow, lagoonward sloping limestone layer on the ocean side can increase freshwater (Bailey et al., 2010). Other factors such as the position of the island relative to wind direction, cross-island grain size differences, and tidal lag also affect the FWL dynamics (Hunt and Peterson, 1980). Larger islands form on the leeward side of atolls and have thicker Holocene deposits and finer sediments because they are not exposed to the large swells and higher energy environment of windward islands (Spennemann, 2006). Numerical model simulations have indicated that the relatively less permeable Holocene deposits on the leeward islands results in K values of about 50 m day^{-1}, while the Holocene sediments on windward islands result in K values as high as 400 m day^{-1} (Bailey et al., 2009). The relatively lower K of the leeward islands results in less tidal propagation and mixing of seawater with the FWL. The lower-energy environment on leeward islands tends to promote a thicker FWL than windward islands. This is evident on Kwajalein Atoll and the thinner FWL on the smaller windward island of Roi-Namur (Gingerich, 1996) as compared to the thicker FWL on the larger, southern leeward Kwajalein Island (Hunt and Peterson, 1980).

In addition to difference in permeability between leeward and windward islands, the cross-island lithology of a given atoll island can contribute to differences in FWL thickness. The lagoon side of a typical atoll island is a relatively low-energy depositional environment protected from big ocean waves where fine Holocene sands are deposited. In contrast, the ocean facing section of an atoll island is a higher-energy depositional environment where coral fragments, and pebble to cobble size sediments have been deposited in the Holocene. In general, sediment size in these unconsolidated Holocene deposits decrease in size from ocean to lagoon similar to what was observed on Majuro atoll by Anthony (1989). It has been demonstrated through time-series monitoring well samples on Kwajalein Island that variations in cross-island lithology affect the rate and extent of tidal propagation, thus affecting the freshwater lens geometry (Hunt and Peterson, 1980). The higher permeability and hydraulic conductivity found on the ocean side promotes faster tidal propagation and increased mixing, and explains the asymmetrical shape of the FWL on atoll islands. For this reason, atoll islands generally have a thicker FWL on the lagoon side as compared to the ocean side.

2.2. Atoll Geochemistry

Typical aquifer geochemistry on atoll islands is dependent on mixing between seawater, recharge water, and their interaction with carbonate source rock; equilibrium and non-equilibrium dissolution-precipitation reactions of aragonite and magnesian-calcite drive the water quality which can be observed through Ca^{2+}, Mg^{2+}, and HCO_3^- concentrations, and the saturation index (SI) and partial pressure of CO_2 (pCO_2) in groundwater (Plummer et al., 1976). Anthropogenic effects on water quality are also a concern on inhabited low-lying atolls and elevated levels of dissolved organic carbon and nutrients are a common indicator of fecal contamination from animal waste (White et al., 2007).

The presence of decaying organic matter derived from plant debris in the soil zone promotes microbial respiration and produces CO_2 pressures in the soil pore water that are as much as two orders of magnitude higher than in rainwater that is in equilibrium with the atmosphere (Plummer et al., 1976). Hydrocarbon contamination can increase microbial activity which also affects natural geochemical processes. A geochemical characterization on Kwajalein Island found that high microbial oxidation of organic matter releases an amount of inorganic carbon nearly equivalent to the amount of carbonate-mineral dissolution (Tribble, 1997). The same study showed that petroleum hydrocarbon contamination increases microbial respiration and mineral dissolution. A hydrochemical investigation at Majuro atoll estimated that 465 m^3 of sediment removal from dissolution reactions resulted in an annual increase in porosity of 0.01% (Anthony et al., 1989). The contrasting inputs to Roi and Namur may help resolve the uncertainty about the extent of human impact and vegetative cover on the FWL and transition zone geochemistry of low-lying carbonate island aquifers.

3.0 Methods

3.1. Field Methods and Groundwater Sampling

Over a two week period in April and May 2015, groundwater samples were collected from a total of 33 monitoring wells from nine separate well clusters located on Roi and Namur (Table 1). Not all of the original U.S. Geological Survey (USGS) well locations (Gingerich, 1996, 1992) were sampled because of time and resource limitations. Therefore, well selection was prioritized so that lagoon and ocean side wells on both lobes of the island are represented and cross island transects could be compared.

The nine well clusters include six on Roi and three on Namur (Fig. 1b); each cluster represents a single location where a group of wells were drilled to discrete depths so that groundwater samples could be obtained along the depth profile of the vertical salinity gradient in the FWL and transition zone. A total of 21 discrete well depths on Roi and 12 discrete well depths on Namur were sampled, ranging from clusters of two to five wells at each location. In Table 1, all wells are identified with the letter 'R' followed by a number that denotes the well cluster and approximate depth below mean sea level of the screen mid-point for each well within each cluster (e.g. R1-1, R1-7, etc.), which is consistent with the original USGS well identification (Gingerich, 1996, 1992). The monitoring wells are constructed of 5.1-cm-diameter poly-vinyl-chloride (PVC) flush-threaded pipe. A 0.61 m section of each pipe is screened 0.15-m from the bottom to allow groundwater to flow into the well only from the desired depths.

All groundwater wells were sampled using protocols of the USGS National Field Manual for the collection of water-quality data (U.S. Geological Survey, variously dated). Using an electrical submersible pump, three wet-casing volumes were purged to remove stagnant water in the well prior to sample collection. A peristaltic pump and nylon tubing was used to lift groundwater to the surface, where it was run through a 0.45 μm filter to remove particulates before being gravity drained into sample bottles. Prior to sample collection at each well, the inside of the nylon tubing was rinsed with well water equivalent to at least two sample volumes to ensure only representative samples from that location and depth were being collected. Chemical preservatives were not used for any collected samples. Sampling procedures were identical for all sample constituents, but sample volume varied from 20 ml vials to 1.0 L bottles depending on the constituent of concern. Samples were placed in a field cooler and transported to a refrigerator for preservation and storage.

A YSI 556 multi-probe handheld multi-parameter field meter was used to measure field water-quality parameters, including pH, temperature, oxidation-reduction potential (ORP), dissolved oxygen (DO), electrical conductivity, and salinity. Total alkalinity was determined for each sample at the end of each field day using the inflection point method by performing multipoint titration with 1.6M H_2SO_4.

3.2. Laboratory Methods

Groundwater samples were analyzed at various laboratories. Major ions and trace elements (except for chloride, bromide, fluoride, and sulfate) were analyzed at the University of Southern Mississippi Center for Trace Analysis using Inductively Coupled Plasma Mass Spectrometry (ICP-MS). The chloride, bromide, fluoride, and sulfate were analyzed using an ion chromatograph (IC), and dissolved inorganic carbon (DIC) and δ^{13}C-DIC were analyzed via continuous flow cavity ring-down spectroscopy following wet chemical oxidation at the USGS in Menlo Park, CA. The nutrient analysis was performed at Woods Hole Oceanographic Institution (WHOI), in Woods Hole, MA using a SEAL AA3 four-channel segmented flow analyzer. The dissolved organic carbon and δ^{13}C-DOC were analyzed using high temperature catalytic con-version DOC analyzer, a GD-100 CO_2 trap and a continuous flow IRMS at WHOI's National Ocean Sciences Accelerator Mass Spectrometry Facility (NOSAMS).

3.3 Water Quality Comparison

To evaluate if water-quality parameters on Roi and Namur are statistically different at the 95% confidence level, median concentrations of selected constituents are compared using a Wilcoxon rank-sum test. The constituents are selected based on the mechanistic hypothesis that the presence of decaying vegetation in the root zone will lead to more microbial oxidation and increased carbonate dissolution through the following reactions:

$$CH_2O + O_2 \rightarrow CO_2 + H_2O \qquad \text{eqn. 2}$$

$$Ca(Mg)CO_3 + CO_2 + H_2O \leftrightarrow 2HCO_3^- + Ca^{2+}(Mg^{2+}) \qquad \text{eqn. 3}$$

The differences in vegetation cover between Roi and Namur may alter the geochemical reactions in equations 2 and 3, which would be observed in the geochemical signal of each lobe. The mechanisms and subsequent geochemical effects are discussed in detail below.

A geochemical study on Kwajalein Island by Tribble (1997) showed that microbial oxidation in the root zone plays an important role in carbonate dissolution on atoll islands. It is reasonable to expect that more vegetative cover would result in greater organic matter input to the soil, thereby producing greater inorganic carbon through microbial oxidation (eqn. 2). The question is whether removal of vegetation on Roi has significantly reduced CO_2 flux in the groundwater and overlying vadose zone, thus reducing dissolution of the carbonate rocks (eqn. 3)?

The inorganic carbon formed by these reactions can either be from microbial oxidation of organic matter (eqn. 2) or carbonate mineral dissolution (eqn. 3). To distinguish whether microbial oxidation (eqn. 2) or carbonate dissolution (eqn. 3) is a greater source of dissolved inorganic carbon (DIC) on each lobe, the measure of $^{13}C/^{12}C$ for DIC ($\delta^{13}C$-DIC) was analyzed. Plants preferentially take up the lighter stable isotope of carbon-12 for photosynthesis and are more depleted in the heavier isotope. Conversely, carbonate minerals are less depleted in the stable isotope of carbon-13 and dissolution reactions produce inorganic carbon with an isotopic signature reflective of the Vienna Pee Dee Belemnite (VPDB) reference standard. Dissolved organic carbon (DOC) in groundwater results from microbial breakdown of leaf litter and other decaying organic matter or from hydrocarbon contamination. I expect that groundwater on Namur may have higher concentrations of DOC due to the larger input of organic litter in the soil zone as compared to Roi.

Carbonate dissolution-precipitation reactions can affect calcium (Ca^{2+}), magnesium (Mg^{2+}), and bicarbonate (HCO_3^-) ion concentrations in carbonate aquifers (Plummer et al., 1976). Therefore, I tested these constituents to evaluate if there is a statistically significant difference in concentration in groundwater on Roi as compared to Namur. If the mechanism for dissolution is related to DIC input, I would expect to observe higher Ca^{2+}, Mg^{2+}, and HCO_3^- concentrations in groundwater related to the dissolution of carbonate minerals.

Nutrient cycling also plays an important role in geochemical processes. Decaying organic matter in the soil is a source of macronutrients, such as nitrogen (N) and sulfur (S). Biological decomposition of organic matter in the soil produces the mineralized form of these nutrients, which are subsequently taken up by plants and/or leached into the groundwater. Under anaerobic conditions, denitrification and sulfate reduction may reduce nutrients to their gaseous form (i.e. NO_3^- to N_2 and SO_4^{2-} to H_2S) where they become unavailable for plant uptake and are released to the atmosphere (Korom, 1992). More vegetative input and microbial oxidation may lead to additional leaching of nutrients in the groundwater, thus I tested for statistically significant difference in concentration of nitrate (NO_3^-), ammonium (NH_4^+), total dissolved nitrogen (TDN), and sulfur (S) in groundwater on Roi as compared to Namur. Similarly, decomposition of organic matter and oxidation reactions influences the pH and oxidation-reduction potential (ORP) of the aqueous system, and thus I tested for statistically significant differences in pH and ORP.

Prior to geochemical reactions with carbonate rocks, groundwater geochemistry is a function of the percent seawater that is mixed with recharge from precipitation or other freshwater sources. Therefore, the groundwater sample concentrations must be normalized by seawater to account for mixing before they can be compared. The mixing of recharge water with seawater in the transition zone results in groundwater concentrations that are a result of conservative and non-conservative reactions. Chloride (Cl^-) does not react readily compared to other major ions, and variations in concentrations of Cl^- in natural waters is primarily due to physical processes (Hem, 1985), thus, the percent seawater that is mixed with recharge in each groundwater sample can be determined using Cl^- concentration and the assumption that all the Cl^- in the groundwater sample originates from seawater. Normalization of the groundwater samples is done by plotting concentrations with respect to percent seawater for both lobes together and calculating a least squares regression line from the combined data set. The residuals for each lobe are then calculated from the regression line and the differences in residuals become statistically comparable. A difference in concentration would be indicated by overall positive residuals on one lobe and negative on the other.

Water quality data typically has non-normal distributions because of infrequent high (or low) values. However, data transformations using successive ladder of powers were attempted to see if the data could be tested under a more robust normal distribution. The transformations did not improve the normal distributions, so a non-parametric test is used for this analysis.

Statistical analysis was performed using the software package JMP version 12.1.0 (SAS Institute, Cary, NC). A Wilcoxon rank-sum test is performed on the distribution of residuals to evaluate whether the median concentrations on Roi and Namur differ,

$$H_o: C_r = C_n \qquad \text{eqn. 4}$$

$$H_a: C_r \neq C_n$$

$$\alpha = 0.05$$

where C_r is the median concentration on Roi and C_n is the median concentration on Namur, and α is the significance level required to reject the null hypothesis (H_o).

The probability of rejecting H_o by chance (false positive) increases when multiple comparisons are done at once (Bonferroni, 1936). Therefore, as a conservative measure, I calculate a Bonferroni experiment-wise error rate for 14 separate parameter comparisons:

$$\alpha_e = 1-(1-\alpha)^k \qquad \text{eqn. 5}$$

where α_e is the experiment-wise error rate (chance of 1 or more false positives), and k is the number of separate parameters to be tested. To compare p-values derived from the Wilcoxon rank-sum test against a tougher significance test which takes into account the higher chance of false positives, a comparison-wise significance level is calculated:

$$\alpha_c = \alpha/k \qquad \text{eqn. 6}$$

where α_c is the new significance level threshold for 95% confidence.

3.4. Geochemical Modeling

To obtain appropriate input concentrations and mixing parameters for thermodynamic modeling, field samples were analyzed for the following constituent groups: major and minor ions, trace metals, nutrients, dissolved organic carbon (DOC), and dissolved inorganic carbon (DIC). The end-member chemistry will be derived from proportions of seawater and rainwater based on the conservative Cl^- concentrations in each sample. Because of difficulty in estimating artificial recharge volume on Roi, MAR water derived from the catchment basin is not accounted for because of the difficulty in estimating the volume recharged and its likely only localized effects. The recharge water is more alkaline and is more concentrated due to evaporation, and may have more organic input from wildlife bathing in the water. But given a net withdrawal of water from the FWL every year on average, and that the artificial recharge would, at most, account for less than 7% of total recharge, the difference in chemistry between rain and artificial recharge is assumed to have negligible effects. However, it is possible that there is some localized effects, especially near well R1 due to its proximity to the recharge area.

Solution concentrations from each groundwater sample were input into the geochemical modeling program PHREEQC (Parkhurst and Appelo, 2013) to obtain charge balance, SI, and pCO_2 values. Within PHREEQC, WATEQ4 was selected as the reference thermodynamic database (Ball and Nordstrom, 1991). Charge balance calculations serve as a check on solute concentrations; the sum of the total cation and anion concentrations require a net charge at or close to zero in order to validate analytical accuracy and check calculations. Generally, the analytical accuracy is considered good if the balance is within ±5 percent error, however, it can be considered acceptable, but less than ideal with ±10 percent error (Hem, 1985).

In the vadose zone and aquifer of carbonate islands, groundwater ion concentrations are affected by the dissolution of calcite and aragonite minerals, which is controlled predominantly by the pCO_2, pH, and alkalinity. Reactions such as dissolution of the carbonate minerals in the groundwater that deviate from conservative freshwater-seawater mixing processes can be identified using thermodynamic modeling. Differences between observed groundwater sample concentrations and theoretical speciation values may indicate a system that has additional chemical inputs from diagenesis or non-equilibrium dissolution-precipitation reactions.

Aragonite and magnesian-calcite are precipitated on atoll reefs and have been shown to be more soluble than pure calcite (Morse and Mackenzie, 1990). Based on core samples and thin sections on Majuro Atoll, the predominant dissolution of aragonite skeletal material followed by minor amounts of calcite and low-magnesian-calcite, indicates a system favoring aragonite dissolution (Anthony et al., 1989). Water flux through the subsurface dissolves source rock, increases secondary porosity, and ultimately results in a net flux of sediment out of the system. Studies have measured dissolution for small carbonate islands and found that water in the FWL and transition zone increases permeability because of diagenetic reactions (Anthony et al., 1989; Plummer et al., 1976). The important driver in this reaction is CO_2 input, which in solution, dissolves carbonate rock (eqn. 3).

The following methods describe how dissolution rates of carbonate minerals in the FWL of Roi and Namur were estimated, including the effects of recharge, inorganic carbon input, and residence times on the rates of the carbonate-diagenetic reactions.

Source rock contributions from carbonate dissolution is determined by measuring excess Ca^{2+}, Mg^{2+}, and HCO_3^- in the system. Given that the only source of these ions is from dissolution of carbonate minerals or seawater, the concentrations in solution that are outside what is expected from conservative rainwater-seawater mixing represent the dissolution of carbonate rock. Therefore, the molar ratios of $Ca^{2+}:Cl^-$, $Mg^{2+}:Cl^-$, and $HCO_3^-:Cl^-$ in local seawater were used to determine the theoretical concentration in each groundwater sample under conservative reactions, and the sum of the excess concentrations of Ca^{2+}, Mg^{2+}, and HCO_3^- represent the mass contribution from dissolution of source rock. Only one sample on Namur (R6-1, Table 1) was within the freshwater lens (<1.3% seawater), so only the excess concentrations for this well were used to calculate dissolution rates and increases in secondary porosity on Namur. Roi has a much larger FWL and I was able to collect five samples (R1-1, R2-1, R3-1, R4-1, and R10-2) that represent FWL concentrations. The average of excess concentrations from the five samples were used to calculate dissolution rate and increases in secondary porosity.

Using numerical simulations, Gingerich (1992) estimated an 84% decrease in recharge on Namur compared to Roi. However, smaller decreases in recharge have been reported in other studies based on empirical calculations of precipitation and ET. Buddemeier and Oberdorfer, (1997), after Falkland (1991), estimated that with 1878 mm of rainfall, an atoll island will have 46% and 25% recharge for 0% and 80% tree cover, respectively. Since the average yearly rainfall on Roi-Namur from 1980-1991 was 1927 mm yr^{-1} (Gingerich, 1992), I use these recharge estimates to calculate dissolution. The empirically derived recharge estimates are used instead of the numerical calculations because they represent a more conservative recharge differential between the two lobes.

It is unknown how much of the water collected in the concrete–lined catchment basin is artificially recharged, therefore, the calculated net recharge on Roi does not take into account the portion of the approximately 30,000 m^3 (about 7% of total estimated recharge to the entire aquifer on Roi) on average of water that is collected in the rainwater catchment and artificially recharged each year. Although there is typically a net withdraw of water from the FWL each year, some percentage of the water collected in the catchment during the wettest months does get artificially recharged and increases the volume of water that percolates through the vadose zone overlying the FWL. Therefore, the flushing rate may be somewhat underestimated in this analysis.

For a qualitative perspective of changes with salinity and depth to source rock concentrations, excess concentrations for the transition zones were also calculated. However, the change in porosity was not calculated for these parts of the aquifer because excess source rock concentrations are more likely to be altered by precipitation reactions at deeper depths.

The thermodynamic equilibrium state of the water will favor precipitation or dissolution of a mineral depending on the temperature, pH, and ionic strengths (Hem, 1985). Solution parameters are used to calculate SI with respect to aragonite using PHREEQC, to determine the favorable thermodynamic direction of the dissolution-precipitation reaction:

$$CaCO_3 + H^+ \leftrightarrow Ca^{2+} + HCO_3^- \qquad \text{eqn. 7}$$

The SI is defined by the equation:

$$SI = \log_{10} IAP/K_{sp} \qquad \text{eqn. 8}$$

where IAP is the ion activity product, and K_{sp} is the solubility constant for the mineral aragonite. A negative SI indicates the favored reaction path is towards dissolution (to the right) and a positive SI favors precipitation (to the left) (eqn. 7). Solutions can then be qualified with respect to a given mineral whether they are saturated (SI=0), supersaturated (SI>0), or undersaturated (SI<0).

As previously mentioned, the primary driver of this dissolution reaction (eqn. 7) is the availability of CO_2 (eqns. 2 and 3), which produces weak acids:

$$CO_2 + H_2O = H_2CO_3\,(aq) \qquad \text{eqn. 9}$$

$$H_2CO_3\,(aq) \leftrightarrow H^+ + HCO_3^- \qquad \text{eqn. 10}$$

$$HCO_3^- \leftrightarrow H^+ + CO_3^{2-} \qquad \text{eqn. 11}$$

Therefore, the concentration CO_2 is an important factor in the subsequent geochemical processes of the aqueous and solid carbonate system. The pCO_2 in groundwater is a volume percentage of CO_2 gas compared to the total gas make-up of that water. Pure water that is exposed to the atmosphere will dissolve CO_2 until it reaches equilibrium with the partial pressure of the surrounding air. Rainwater in equilibrium with the atmosphere will have a pCO_2 of approximately $10^{-3.4}$ or 0.04% Vol CO_2 (400 ppm), which is equivalent to 0.0004 atm (1 atm=1.0133×10^5 Pa). The log pCO_2 is the unit used to express CO_2 concentrations (e.g. rainwater has a log pCO_2 of -3.4). In groundwater systems, values of pCO_2 of $10^{-2.5}$ to $10^{-1.0}$ have been observed (Hem, 1985), which is one to three orders of magnitude greater concentrations than in rain. Plummer and others (1976) found similarly elevated pCO_2 concentrations in soil pore water samples. This is because plant decay and microbial respiration in the top soil, especially prevalent in tropical climates with heavy vegetation, supply an influx of CO_2 into solution as water travels vertically through the soil profile and into the aquifer.

Studies have shown there is a moderate trend of increased dissolution of carbonate minerals with increasing pCO_2 (Anthony et al., 1989; Plummer et al., 1976). Respiration and aerobic decay has been shown to increase pCO_2 (eqn. 2), which in turn reduces the pH (eqns. 10–12), and reduces saturation and carbonate concentrations of water (Drever, 1988). On Kwajalein Island, Tribble (1997) showed that the predominant reaction in the system was the dissolution of calcium carbonate driven by CO_2 from microbial respiration. If exposure time to sediments is sufficient during water flux in the vadose zone, carbonate dissolution proceeds and Ca^{2+}, Mg^{2+}, and HCO_3^- is transported to the groundwater where thermodynamically favored reactions continue.

4.0 Results

4.1. Freshwater Lens Asymmetry

The shape of a typical FWL on atoll islands is asymmetrical with a thicker FWL found on the lagoon side (Ayers and Vacher, 1986; Hunt and Peterson, 1980). Greater hydraulic conductivity on the ocean side increases tidal efficiency, which increases the dispersion of more saline waters through the upper aquifer. As a result, the transition zone becomes thicker on the ocean side but the FWL is truncated at shallower depths compared to the lagoon side. Roi has a significantly thicker FWL on the ocean side along with a thicker transition zone (Fig. 3a–b). In contrast, the FWL and transition zone on Namur exhibits a classic asymmetric shape with a slightly thicker lens on the lagoon side (Fig. 3c). The observation of a thicker FWL on the ocean side of Roi would be an unlikely scenario in a natural atoll aquifer, especially one that is on a windward island. It seems that the influx of additional recharge as result of reduced ET and MAR has significantly reshaped the FWL on Roi.

Bailey and others (2008) used numerical models to show that recharge values of 1.25, 2.00, and 2.75 m yr^{-1} on an atoll increased the FWL thickness and that the FWL could be truncated by the Thurber Discontinuity. However, the geometry of the FWL did not significantly change. Drilling records on Roi-Namur indicate there is a hard consolidated layer located 7–17 m bls (Gingerich, 1992), but the thicker FWL located on Roi is only 3 m and 5 m thick on the lagoon and ocean side, respectively (Fig. 3a–b). The depth of the Thurber Discontinuity may vary from ocean to lagoon side, but it is unlikely to favor a thicker FWL on the ocean side because the geology of most atolls have thicker Holocene deposits on the lower-energy lagoon side as observed on Enewetak Atoll (Buddemeier, 1981) and Majuro Atoll (Anthony et al., 1989).

The more likely reason for the unexpected FWL geometry on Roi is the focused recharge on certain parts of the island. If recharge was equally distributed across the island, lithologic influences would certainly limit mixing on the lagoon side, forming a thicker lens there. The location of recharge on Roi is important because it is linked to the hydraulic gradient and flow direction of groundwater in the upper aquifer. Groundwater level contours developed by Gingerich (1996) shows the likely groundwater flow direction on Roi and Namur (Fig. 4). The highest head on Roi is located in the eastern part of the lobe approximately half-way between the ocean and lagoon side under the concrete-lined catchment basin. The concrete-lined catchment covers a large area of the eastern section and lagoon side of Roi and essentially eliminates recharge directly underneath it. Although recharge is limited by the paved surfaces, groundwater head is highest and FWL is still relatively thick under the concrete-lined catchment. This is likely due to lithologic influences where relatively low hydraulic conductivity limits tidal mixing and freshwater drainage and builds head. The general flow direction in the FWL on Roi radiates from the highest head in the center outward in all directions. The water level map on Namur nearly mirrors that of Roi. The similar head contours exist even though Namur is not as paved, indicating that lithological influences are more influential than recharge location in determining groundwater head and hydraulic gradients.

The MAR system on Roi reroutes rain that would normally fall over the concrete-catchment and artificially recharges that water over the grassy area adjacent to the runway and between wells R1 and R2. This focused artificial recharge has produced the thickest part of the FWL under well R1 even though it is on the ocean side (Fig. 3a). It is evident from the groundwater level map that freshwater recharged over the grassy area adjacent to the runway will flow downgradient towards the ocean side of the island, with the strongest gradients favoring flow towards wells R4 and R10 and producing a thick FWL (Fig. 3b). Even with a thick FWL and preferential flow towards the ocean side, groundwater head has not built up accordingly. This may partly be explained by the coarser sediments that allow freer drainage of freshwater on the ocean side but do not allow for build-up of head. A freshwater distribution similar to Roi was observed on Enjebi Island by Buddemeier and Oberdorfer (1997); they suggested that the impervious reef plate on the ocean side may reduce water flux to the ocean and increase supply, or additionally, that some areal recharge is redirected towards the center of the island over the lagoon sloping reef plate. However, these explanations do not sufficiently explain the lower than expected head based on the Ghyben-Herzberg relationship. Assuming that the 50% isochlor is the GHD, then the head at well R10 should be approximately 0.28 m (0.9 ft). However, the observed groundwater head is only 0.05 m (0.17 ft). It remains unclear what the underlying mechanism is that allows the FWL to be thicker on the ocean side without increasing head.

Overall, a large amount of water that would have been recharged on the lagoon side has been diverted and recharged on the ocean side and in an area that favors groundwater flow towards the ocean, which helps explain the unexpected asymmetry of the FWL. It is likely that without the LULC modifications and MAR on Roi, the FWL geometry would reflect a more typical atoll aquifer, similar to what is observed on Namur.

4.2. Water Quality Comparison

Statistically significant differences ($\alpha = 0.05$) were found for pH, ORP, Ca_{2+}, NH_4^+, TDN, and $\delta^{13}C$-DIC in groundwater of Roi and Namur (Table 2, Fig. 5a-f). Alkalinity, DO, S, HCO_3^-, Mg^{2+}, NO_3^-, DIC, and DOC in groundwater of Roi and Namur are not statistically different at $\alpha=0.05$ (Table 2).

Ca^{2+} and pH. Lower pH values and higher concentrations of Ca^{2+} are observed on Namur, indicating relatively more acidic groundwater and greater dissolution of carbonate minerals.

DIC. Groundwater on Namur is depleted in $\delta^{13}C$-DIC relative to groundwater on Roi (Fig. 5c), indicating there is a relatively larger fraction of DIC on Namur from microbial oxidation of organic matter than from dissolution reactions as compared to Roi. However, the DIC concentrations are not statistically higher on Namur even with higher dissolution rates (see section 4.3), which suggests that there is another source of inorganic carbon on Roi that is not sourced from decaying vegetation. Upon closer observations of DIC concentrations, wells R3 and R4 on Roi have elevated concentrations of DIC which correlate with elevated levels of pCO_2 and nutrients and may be an indication of fecal contamination (Fig. 6).

Nutrients and ORP. I originally hypothesized that greater organic matter and microbial respiration in the soil zone will consumes oxygen, and therefore recharge on the more densely vegetated Namur would have a more reduced groundwater than Roi. However, the data shows a significantly more reduced (Fig. 5d) groundwater on Roi which is likely a result of elevated concentrations of NH_4^+ (Fig. 5f) in groundwater on Roi. The landscape on Roi is not fertilized. It's likely that point source contamination associated with human activities are the source of elevated nutrients in the groundwater on Roi. NH_4^+ is found in human and animal waste and elevated concentrations are often found in groundwater near septic systems and leaky sewage pipes. There are three actively used septic tanks and leach fields on Roi-Namur; one is located on the dredge-filled, conjoined section of the island that is adjacent to well R3, and two are located on Namur.

Most of the highest concentrations of NH_4^+, NO_3^-, and TDN occur in the same cluster of wells. Specifically, wells at R3 on the lagoon side and R4 on the ocean side have some of the highest concentrations (Fig. 6). Well R3-1 has the second highest NO_3^- concentration but NO_3^- is not detected at deeper depths where NH_4^+ concentrations tend to increases. The shallow wells at R4 (R4-1, R4-4, R4-7) have high NO_3^- concentrations, and NH_4^+ increases with depth but not nearly as much as wells at R3. The generally increasing NH_4^+ and decreasing NO_3^- concentrations with depth indicates dissimilatory nitrate reduction to ammonium (DNRA) may be occurring in deeper parts of the well where oxygen is typically low (Korom, 1992). The smaller increase in NH_4^+ and more persistent NO_3^- concentrations with depth at well R4 compared to well R3 may be a result of faster water flux and low residence time on the ocean side which transports NO_3^- and limits DNRA. This explains the relatively lower ORP found on Roi. Unlike well R3, well R4 is not located near any septic systems so it is unclear why nutrient concentrations are elevated at this location. There is likely some point source contamination nearby related to leaky pipes or other operations on the island near R4.

The higher ORP is also consistent with a relatively lower pH. The vegetation signal in Namur groundwater is clear based on the depleted δ^{13}C-DIC values, and along with the lower pH, indicates that DIC input into groundwater from microbial respiration in the root zone is probably greater on Namur. Although Ca^{2+} is statistically higher on Namur, DIC concentrations are not statistically different. Along with the contamination from animal waste, there is likely some effect from MAR water on Roi. MAR water exhibits higher pH (9.48) and elevated DOC which would promote CO_2 production, but the more alkaline water may buffer the groundwater and limit dissolution on parts of Roi.

Statistical Significance. If this study had embarked on a mission to find any possible geochemical perturbations of 14 random parameters without an underlying methodology for choosing these parameters, then the experiment-wise error rate for a false-positive finding would be 0.49. The comparison-wise significance level for 14 comparisons would be α =0.0036. With this more conservative confidence level, the differences found in NH^{4+} and $\delta^{13}C$-DIC are the only ones unlikely to occur just by chance. The other previously described results do not meet this more conservative confidence level, however, they are potentially valid due to the varying hydrochemical inputs and underlying geochemical reactions that are affected as proposed by the mechanistic hypotheses.

4.3. Carbonate Dissolution

Calculated source rock contributions (SRC) from the FWL and overlying vadose zone indicate that more dissolution is occurring on Namur (Table 3a). However, with a larger FWL and overlying vadose zone, and greater flushing, the total sediment removal on Roi is 72 m^3 yr^{-1} compared to Namur 20 m^3 yr^{-1} on Namur. Using the estimated recharge for each lobe, the area underlain by a FWL, the volume of the FWL, a rock density of 2.5 kg/m^3, and assuming an effective porosity of 0.3, the estimated annual increase in porosity is 0.002% on Roi and 0.014% on Namur. The annual increase in porosity in the FWL and overlying vadose zone on Namur is approximately seven times greater than Roi, which indicates that the dissolution of carbonate rock (increase in annual porosity) has been reduced as a result of LULC change and MAR.

It is more difficult to estimate the changes in dissolution rate and porosity in deeper, more saline parts of the aquifer because dissolved minerals can be transported from shallower depths. However, using a similar method as the FWL calculations, average SRC calculations from deeper depths can be made to estimate changes in excess ion concentrations with depth and increasing salinity. The SRC for three different seawater mixes are calculated: <1.3%, 1.3–50%, >50% (Table 3b). As stated previously, the greatest dissolution rates on Namur occur in the FWL (<1.3% seawater). On Namur, the transition zone from 1.3–50% has a smaller average SRC than in the FWL. The opposite pattern is observed on Roi, where the transition zone has greater average SRC than in the FWL. The average SRC decreases for both lobes at the greatest seawater mixtures (>50%), either as a result of tidal flushing and removal of dissolved sediment and/or non-equilibrium reactions as a result of mixing. The lower dissolution rates in the FWL and overlying vadose zone on Roi are likely a result of relatively greater flushing due to increased recharge.

The saturation indices on Roi and Namur are consistent with what I would expect given the SRC calculations. The groundwater at low and intermediate salinities in Roi are undersaturated with respect to aragonite and become supersaturated at the most saline depths (Fig. 7). This indicates that undersaturated water is being transported from the FWL on Roi to deeper depths where dissolution persists. Most groundwater samples on Namur stay close to saturation throughout the profile. Groundwater reaches equilibrium conditions in the FWL before being transported deeper in the aquifer. Geochemical processes are explored further through geochemical modeling in the next section.

4.4. Equilibrium/Non-equilibrium Reactions

The equilibrium/non-equilibrium dissolution-precipitation reactions in carbonate aquifers are described in this study using the SI with respect to aragonite and pCO_2 of groundwater. Plummer (1976) ascribed changes in SI of groundwater in carbonate aquifers to five possible factors: variability in soil pCO_2, evasion of CO_2 through the soil zone, CO_2 flux in the phreatic zone, dissolution-precipitation non-equilibrium reactions of carbonate minerals, and seawater mixing. To investigate how geochemical processes have been altered on Roi due to the MAR operation and LULC changes, I analyze these factors and compare to processes on Namur using geochemical modeling.

Soil pCO_2 and CO_2 Evasion. For this study, I assume a closed system exists once water enters the phreatic zone, and CO_2 flux is only caused by dissolution or mixing process that transport groundwater to sea. There is enough soil cover to limit any CO_2 evasion and there is no direct sources of additional CO_2 input in the groundwater such as may occur from marshes. This is a reasonable assumption since it was observed on Kwajalein Island that most of the production of CO_2 by microbial oxidation occurs in the vadose zone or near the top of the water table (Tribble, 1997).

Groundwater CO_2 Flux. The only FWL sample collected on Namur is from well R6-1, and it has the greatest log pCO_2 (-1.51) of either lobe (Fig. 8). The log pCO_2 of the FWL samples on Roi range from -2.52 to -1.53. There is apparently more CO_2 in the FWL and shallowest parts of Namur. On Roi, the lowest pCO_2 concentrations occur in the most saline wells (>80% seawater) (Fig. 8) and at the shallowest well at site R3 (Fig. 6). pCO_2 values in the most saline groundwater on Namur trends higher than Roi.

Although the overall DIC concentrations in groundwater on Roi and Namur are not statistically different, there is a difference in the DIC profile when the two lobes are compared (Fig. 9). The shallowest sections of the aquifer on Namur generally have greatest amount of DIC and concentrations decrease with depth. In contrast, the shallowest sections of the aquifer on Roi generally have lower DIC concentrations (5.00–5.99 mg C/L) and there is an increase in concentrations (<6.00) in parts of the intermediate transition zone. There is an apparent shift to greater DIC concentrations deeper in the profile on Roi compared to Namur.

The differences in DIC depth profiles may be attributed to the lower residence times and more rapid flushing rates of groundwater on Roi than Namur, which promotes more dissolution deeper in the profile on Roi. The low pCO_2 at well R3-1 may be related to the elevated NO_3^- concentrations from a nearby leach field. It is likely that nutrients are predominantly in the form of NO_3^- in the shallowest well where sufficient oxygen is present (3.4 mg/L). The next deepest well (R3-4) has elevated NH_4^+, a spike in TDN, and an increase in DOC, DIC, and pCO_2. A reducing environment at this depth favors NH_4^+. Also, most of the mass from the contamination plume may be flowing closer to this depth since TDN concentrations and NH_4^+ concentrations have spiked. Wells R4-1, 4-4, and 4-7 also have elevated NO_3^-, TDN, DOC, DIC, and pCO_2, but NH_4^+ concentrations are low or not detected (Fig. 6). The source of nutrients at this location is unknown since well R4 is not located near any septic systems, but the lack of NH_4^+ may indicate a non-organic source of nitrogen, leaky pipes, or possibly a lack of mineralization due to low residence times as a result of a large recharge flux.

Non-equilibrium Reactions. The FWL on Roi is generally undersaturated with respect to aragonite (Fig. 7), which indicates that the residence time of the water in the FWL is shorter than the rate of equilibrium reactions. This is likely a result of more recharge and greater water flux through the groundwater system, which allows for discharge of freshwater out of the system at a relatively faster rate. By contrast, the FWL on Namur is saturated with respect to aragonite, indicating that longer residence times on Namur play a part in increasing dissolution as evident by water that is closer to equilibrium and has greater average SRC.

Seawater Mixing. When seawater mixes with carbonate groundwater the resulting SI may differ depending on the pCO_2 and SI of the original FWL groundwater (Matthews, 1971). A mixture of supersaturated and/or saturated waters can produce undersaturated water (Thrailkill, 1968; Wigley and Plummer, 1976), and the mixture of two undersaturated waters can produce supersaturated water (Runnells, 1969). A theoretical mixing line for carbonate groundwater and seawater is produced with PHREEQC for both Roi and Namur to predict the chemistry of groundwater under a mixing only scenario (Fig. 10). The actual groundwater SI is transposed on the plots and the data indicates that water on Roi follows the non-linear theoretical curve reasonably well, and a polynomial function best fits the data with an R^2 value of 0.43 (Fig. 10a). This indicates that groundwater-seawater mixing is a dominant geochemical process on Roi. Conversely, SI values from Namur do not align with the theoretical curve (Fig. 10b), but generally remain close to equilibrium (0±0.2 SI). Groundwater on Roi skews towards unsaturated waters at lower seawater percentage and supersaturated water at mixtures containing predominantly seawater (>75%).

On Roi, there is a strong negative trend of supersaturation with decreasing pCO_2 compared to a weak trend on Namur (Fig. 11). The supersaturated conditions and low pCO_2 from deep sections of the aquifer on Roi resemble chemistry closer to that of seawater (SI=0.68, log pCO_2=-3.45). On the other hand, most of the aquifer on Namur is relatively close to saturation with respect to aragonite, and deep wells have higher pCO_2. A larger flux of water through the aquifer and observations of undersaturated water in the FWL indicate shorter residence times of groundwater on Roi. Mixing of seawater and carbonate groundwater is greater as a result of the increased recharge and flux through the system, and consequently, residence time in the aquifer on Roi is reduced. Less recharge on Namur means less flushing occurs and slower mixing processes increases residence time, as indicated by waters that are closer to saturation with respect to aragonite. The higher pCO_2 and saturated or slightly under-saturated conditions in deep wells on Namur indicates processes other than mixing are dominant. CO_2 transport out of the system is occurring at a significantly slower rate and the kinetics of equilibrium and non-equilibrium dissolution-precipitation reactions is a more dominant geochemical process.

5.0 Summary

Modifications to LULC and MAR on Roi have altered natural recharge patterns. Greater tidal efficiency on the ocean side typically limits the FWL volume relative to the lagoon side. However, the influx of water from MAR and relatively lower ET on Roi has increased recharge and increased freshwater volume and FWL thickness on the ocean side. These findings indicate that the ocean side of atoll aquifers have the capacity for additional storage, but location is an important factor to consider in implementing an MAR system and/or installing pavement and buildings. Although the ocean side is able to store more water, as we observed, results suggest that the FWL on the lagoon side can become thicker and may be more efficient in storing freshwater because it has less tidal mixing and relatively slower drainage compared to the ocean side. The area directly under the catchment basin on Roi-Namur may have the greatest capacity to store water due to its central location and preferable lithologic influence on groundwater storage.

Statistical analysis of the selected groundwater quality parameters identified six that differed between the contrasting lobes. The geochemical mechanisms responsible for these differences are inter-related, but the findings indicate that the flow and reaction dynamics are complicated. Depleted δ^{13}C-DIC, lower pH, and higher Ca^{2+} suggest decay of vegetation and increased microbial respiration is responsible for the higher dissolution rate on Namur. The annual increase in porosity in the FWL and overlying vadose zone is 0.002% on Roi and 0.014% on Namur. At the same time, greater dissolution of aragonite and magnesian-calcite should theoretically produce more Mg^{2+} and inorganic carbon species, and consequently, differences in alkalinity and HCO_3^-. However, statistically significant differences were not observed for these parameters. These unexpected findings are likely related to contamination from human activities on the island, chemically altered recharge water from the MAR system, and increased groundwater flux and reduced residence time.

Observations of individual well concentrations provides more insight into the responsible geochemical processes. High DIC concentrations at wells R3 and R4 correlate with elevated pCO_2 and nutrient concentrations. Therefore, changes in water quality parameters due to LULC change are masked by geochemical processes related to contamination from human activity.

There is considerable evidence that residence time is reduced on Roi due to the large influx of water and strong flow gradient towards the more permeable ocean side.

Dissolution rates are higher in the FWL on Namur and the water is saturated with respect to aragonite. In contrast, most shallow wells on Roi have groundwater that is undersaturated with respect to aragonite, which indicates that the residence time is slow relative to the reaction rate for carbonate dissolution. Undersaturated waters are transported and persist deeper in Roi, and SRC calculations indicate some dissolution has been shifted to the intermediate transition zone. In the deepest wells on Roi, the SI becomes supersaturated with respect to aragonite, and has characteristics more similar to seawater. These observation help confirm a mixing-dominated signal in Roi groundwater and the low pCO_2 at deeper depths on Roi are also consistent with this interpretation. In contrast, longer residence times on Namur allow equilibrium reactions to take place over a longer period time, while less mixing reduces CO_2 transport out of the system. This is indicated by higher pCO_2 in general and groundwater that is close to saturation with respect to aragonite at most depths.

6.0 Conclusion

The reduction in vegetation and the implementation of an MAR system on Roi has successfully increased potable groundwater supply. The LULC practice has altered natural geochemical reactions and reduced dissolution rates in the FWL without detrimental effects to the overall groundwater quality. Contamination from human activities poses the greatest threat to water quality, but this can be mitigated by a groundwater management plan that emphasizes oversight of this limited and vulnerable resource. As climate stressors continue to strengthen and population growth increases demand for water resources, water managers throughout the thousands of populated low-lying carbonate islands in the world should consider LULC change and MAR as a viable method to reduce ET, enhance recharge, and increase groundwater supply.

7.0 Tables

Table 1. Field parameters and concentrations of selected groundwater constituents from samples collected on Roi-Namur in April – May 2015.

well or sample ID	sample date	sample time	temperature (°C)	pH	ORP (mV)	dissolved oxygen (mg/L)	conductivity (mS/cm)	alkalinity (mg/L $CaCO_3$)	Ca^{2+} (mmol/L)	Cl^- (mmol/L)	Mg^{2+} (mmol/L)
R1-1	5/2/2015	8:47	28.94	7.65	11.4	3.43	0.53	173.9	1.14	1.12	0.89
R1-7	5/2/2015	9:23	29.41	7.70	-87.4	2.36	5.50	241.6	2.47	48.84	5.89
R1-12	5/2/2015	10:19	29.30	7.60	-143.0	2.73	29.94	216.3	6.92	293.68	30.88
R2-1	5/2/2015	12:10	29.13	7.45	2.0	1.45	0.74	246.7	1.74	1.86	1.22
R2-4	5/2/2015	12:48	29.42	7.61	-132.7	1.55	11.69	236.6	3.79	96.60	10.19
R2-7	5/2/2015	13:20	29.18	7.60	-186.3	1.13	36.47	178.2	8.29	362.58	37.34
R2-12	5/2/2015	13:55	29.07	7.63	-190.1	1.23	44.02	147.6	9.26	442.97	43.96
R2-16	5/2/2015	14:40	29.03	7.60	-163.7	1.46	46.51	162.8	9.65	469.60	47.94
R3-1	5/4/2015	17:52	29.11	7.92	-66.2	3.40	0.67	-	1.52	2.22	0.78
R3-4	5/4/2015	13:28	31.04	7.50	-199.6	2.15	24.65	334.6	6.80	227.25	26.33
R3-7	5/4/2015	15:48	30.17	7.56	-218.9	1.56	25.94	250.7	9.19	405.72	43.10
R3-11	5/4/2015	14:57	30.33	7.60	-207.5	3.20	46.38	203.2	9.92	472.54	49.60
R3-16	5/4/2015	16:52	29.86	7.65	-209.6	2.42	47.66	183.0	10.32	484.50	51.50
R4-1	5/6/2015	15:06	29.71	7.52	-26.2	4.22	0.67	258.8	2.28	1.09	0.62
R4-4	5/6/2015	16:37	30.12	7.46	-34.4	2.85	2.80	306.9	2.81	18.28	2.50
R4-7	5/6/2015	17:09	29.56	7.42	-31.4	1.86	16.81	270.9	4.88	152.60	16.22
R4-11	5/6/2015	17:33	28.98	7.55	-144.5	2.15	35.15	223.4	7.56	344.44	35.35
R4-16	5/6/2015	17:55	28.71	7.52	-107.1	1.55	44.61	-	9.45	450.28	47.24
R5-1	5/6/2015	9:15	29.51	7.57	-142.5	2.07	25.95	281.1	5.72	180.95	20.23
R5-4	5/6/2015	10:06	29.90	7.64	-159.8	3.35	42.35	-	9.50	424.84	44.33
R5-7	5/6/2015	10:40	29.54	7.65	-167.6	1.05	42.58	165.8	8.95	431.64	42.59
R5-12	5/6/2015	11:20	29.50	7.62	-130.8	1.50	46.79	165.3	10.10	479.35	50.58
R5-12 d	5/6/2015	11:50	29.75	7.64	-128.4	1.73	47.15	-	10.85	474.92	54.40
R5-16	5/6/2015	12:35	29.46	7.59	-98.2	1.81	49.60	159.2	10.41	509.11	53.31
R6-1	5/1/2015	9:40	29.82	7.46	48.3	3.14	1.71	321.0	2.41	6.97	1.87
R6-4	5/1/2015	10:38	29.85	7.46	-134.9	1.38	19.79	313.0	6.25	180.67	19.02
R6-6	5/1/2015	11:28	29.66	7.45	-116.3	1.41	33.20	242.7	7.99	322.83	33.23
R6-11	5/1/2015	12:12	29.38	7.42	-65.3	1.58	39.86	200.2	9.13	398.34	41.75
R6-16	5/1/2015	13:15	29.14	7.48	-69.6	1.27	44.47	171.8	9.43	449.46	47.08
R7-3	4/30/2015	18:23	29.07	7.31	6.0	3.88	19.10	-	5.23	173.43	17.64
R7-6	4/30/2015	18:55	29.07	7.32	-3.3	2.08	24.12	-	6.46	223.84	23.74
R9-8	5/2/2015	18:22	28.55	7.57	-213.8	0.69	47.09	187.0	10.21	477.14	51.33
R9-8 d	5/2/2015	18:52	28.47	7.65	-209.8	0.45	46.89	-	10.13	480.13	50.48
R10-2	5/7/2015	8:20	29.53	7.60	-7.8	3.64	0.77	246.3	1.62	2.03	1.31
R10-6	5/7/2015	8:50	29.50	7.71	-95.9	2.93	6.55	281.4	2.08	51.78	6.78
seawater	5/7/2015	13:30	29.69	8.10	-47.8	4.95	52.83	114.2	10.44	546.89	55.73
seawater d	5/7/2015	14:00	29.45	8.07	-42.8	3.65	52.92	-	10.65	544.75	54.31
rain	6/27/2015	14:00	22.10	6.50	-	-	0.01	3.2	0.01	0.05	0.01
catchment	5/4/2015	17:30	32.29	9.48	-50.9	6.87	0.08	-	0.17	0.20	0.04
field blank	5/6/2015	8:45	27.03	5.73	45.1	6.00	0.00	-	ND	0.16	0.00

Note: N/A indicates concentrations are too low for accurate analysis; ND indicates concentrations are below detection limit; "-" symbol indicates that sample was not analyzed for given parameter; "d" after well number indicates duplicate sample.

Table 1 continued.

well or sample ID	NH_4^+ (mmol/L)	NO_3^- (mmol/L)	TDN (µmol/L)	S (mmol/L)	DIC (mmol C/L)	$\delta^{13}C_{VPDB}$-DIC (‰)	DOC (µmol/kg)	charge balance	saturation index (aragonite)	log pCO_2	% seawater based on Cl^- concentration
R1-1	4.32E-04	1.09E-03	14.357	0.04	3.83	-9.90	253.97	5.94	-0.29	-1.92	0.20
R1-7	1.61E-03	0.00E+00	7.445	2.81	5.50	-6.50	112.48	2.66	-0.32	-1.64	8.93
R1-12	7.61E-03	2.19E-04	20.638	15.60	4.83	-5.30	85.57	-3.02	-0.29	-1.71	53.70
R2-1	6.71E-04	0.00E+00	13.233	0.25	5.50	-9.20	209.63	4.88	-0.06	-1.72	0.34
R2-4	1.52E-03	0.00E+00	13.290	5.71	5.25	-4.70	163.32	3.17	-0.2	-1.73	17.66
R2-7	2.52E-02	0.00E+00	37.279	20.34	5.50	-9.20	81.54	-3.30	-0.38	-1.77	66.30
R2-12	2.65E-02	6.54E-04	42.792	24.54	2.91	-2.90	56.48	-3.32	0.26	-2.62	81.00
R2-16	2.55E-02	0.00E+00	36.726	24.35	3.16	-3.60	51.89	-0.65	0.4	-2.7	85.87
R3-1	1.43E-03	5.61E-02	85.162	0.18	4.16	-11.00	69.82	2.15	0.53	-2.52	0.41
R3-4	4.39E-02	0.00E+00	871.973	12.46	6.99	-4.80	157.97	5.33	0.25	-1.83	41.55
R3-7	5.94E-02	0.00E+00	85.083	23.66	4.91	-4.10	104.63	-2.02	0.56	-2.44	74.19
R3-11	3.97E-02	0.00E+00	58.699	26.94	4.00	-4.20	78.75	-0.33	0.41	-2.48	86.40
R3-16	8.23E-02	0.00E+00	123.408	27.82	3.58	-3.80	76.78	0.97	0.4	-2.57	88.59
R4-1	0.00E+00	3.00E-02	105.370	0.13	6.00	-8.60	323.21	4.97	-0.04	-1.55	0.20
R4-4	3.03E-04	6.17E-02	120.115	1.34	6.99	-10.50	227.13	3.60	-0.02	-1.52	3.34
R4-7	0.00E+00	3.10E-02	31.702	8.26	6.08	-5.10	119.51	3.42	-0.2	-1.62	27.90
R4-11	1.12E-02	0.00E+00	18.952	18.54	4.83	-4.00	70.32	-3.92	-0.16	-1.83	62.98
R4-16	5.42E-03	0.00E+00	9.579	25.52	3.41	-3.60	40.43	-1.07	0.18	-2.42	82.33
R5-1	4.24E-03	0.00E+00	18.109	11.10	6.24	-10.50	144.78	5.55	-0.14	-1.63	33.09
R5-4	2.47E-02	0.00E+00	41.282	24.25	3.83	-5.20	71.03	-1.36	0.37	-2.47	77.68
R5-7	2.54E-02	0.00E+00	41.196	21.75	3.58	-4.60	67.50	-2.55	-0.27	-1.94	78.93
R5-12	1.49E-02	0.00E+00	24.888	27.37	3.41	-4.40	51.56	-0.03	-0.03	-2.19	87.65
R5-12 d	1.45E-02	0.00E+00	23.186	29.21	3.33	-4.30	52.75	3.99	0.34	-2.56	86.84
R5-16	5.16E-03	1.71E-04	14.470	28.96	3.33	-3.70	53.80	-0.06	-0.13	-2.12	93.09
R6-1	1.26E-03	3.90E-03	13.080	0.74	7.33	-13.90	155.73	5.75	0.02	-1.51	1.27
R6-4	1.68E-03	0.00E+00	6.224	9.87	6.66	-10.80	110.02	4.10	0.16	-1.78	33.03
R6-6	2.07E-03	0.00E+00	10.462	17.52	5.16	-9.10	76.29	-3.39	0	-1.87	59.03
R6-11	4.88E-03	3.84E-04	17.336	22.24	4.25	-7.40	56.40	-1.79	-0.08	-1.96	72.84
R6-16	6.11E-03	0.00E+00	27.806	25.40	3.66	-4.70	45.87	-1.14	-0.2	-1.99	82.18
R7-3	1.99E-03	4.15E-03	11.853	9.78	5.83	-12.40	88.34	1.48	0.1	-1.91	31.71
R7-6	1.09E-03	8.12E-03	15.588	13.03	5.75	-12.10	80.33	3.92	0.14	-1.94	40.93
R9-8	5.63E-02	0.00E+00	118.509	27.77	3.75	-3.60	63.25	0.40	0.24	-2.39	87.25
R9-8 d	5.74E-02	0.00E+00	119.865	27.46	3.66	-3.50	60.49	-0.94	0.35	-2.52	87.79
R10-2	1.40E-03	9.13E-03	34.480	0.25	5.58	-7.60	142.18	4.81	-0.15	-1.65	0.37
R10-6	2.86E-03	0.00E+00	16.531	2.78	6.33	-4.60	130.07	3.04	-0.3	-1.61	9.47
seawater	7.26E-04	3.13E-04	12.825	30.27	2.00	-1.00	66.51	-0.79	0.68	-3.45	100.00
seawater d	7.41E-04	3.22E-04	12.278	28.74	0.00	-	64.88	-0.79	N/A	N/A	99.61
rain	-	0.00	-	0.00	0.19	-	-	N/A	-5.11	-2.44	0.01
catchment	8.00E-04	1.91E-03	26.671	ND	0.25	-	246.49	9.07	0.04	-5.32	0.04
field blank	1.56E-03	8.27E-05	3.191	ND	0.03	-	32.68	N/A	N/A	N/A	0.03

Note: N/A indicates concentrations are too low for accurate analysis; ND indicates concentrations are below detection limit; “-” symbol indicates that sample was not analyzed for given parameter; “d” after well number indicates duplicate sample.

Table 2. Median concentrations of Roi and Namur groundwater chemistry are compared using a Wilcoxon rank-sum test to see if there is a statistically significant difference in concentrations. H_0 is rejected at $\alpha=0.05$.

Results of Wilcoxon Rank-Sum Test

parameter	**p-value**	**lobe with higher concentration when H_0 is rejected**
Ca^{2+}	0.04	Namur
$\delta^{13}C$-DIC	<0.01	Roi (more depleted)
NH_4^+	<0.01	Roi
ORP	0.01	Namur (less reduced)
pH	0.05	Roi
TDN	0.03	Roi
alkalinity	0.27	
DIC	0.76	
DO	0.82	
DOC	0.20	
HCO_3^-	0.57	
Mg^{2+}	0.85	
NO_3^-	0.77	
S	0.35	

Note: parameters include dissolved inorganic carbon (DIC), dissolved oxygen (DO), dissolved organic carbon (DOC), total dissolved nitrogen (TDN), and oxidation-reduction potential (ORP).

Table 3. (a) Dissolution rate from FWL (≤1.3%) calculated using recharge, surface area underlain by freshwater lens, and source rock contribution (SRC). (b) SRC calculations for transition zones on Roi and Namur.

a) Dissolution Rate Calculations

parameters for dissolution calculation	**Roi**	**Namur**
rainfall (mm/yr)	1927	1927
recharge (mm/yr)	886	482
surface area underlain by freshwater lens (km^2)	0.46	0.14
flushing (L/yr)	4.08E+08	6.74E+07
source rock contribution (kg/L)	3.09E-04	5.08E-04
source rock flushed (kg/yr)	1.26E+05	3.43E+04
volume dissolved (m^3/yr)	72	20
annual increase in porosity (%)	**0.002**	**0.014**

b) Calculated Source Rock Contribution (SRC)

	Ca^{2+} (mmol/L)	**Mg^{2+} (mmol/L)**	**HCO_3^- (mmol/L)**	**Avg SRC (mmol/L)**
≤1.3% seawater				
Roi	1.63	0.80	3.68	6.10
Namur	2.28	1.16	6.37	9.81
1.3–50% seawater				
Roi	1.91	1.21	4.89	8.00
Namur	2.29	0.59	5.18	8.06
>50% seawater				
Roi	1.05	0.99	2.16	4.21
Namur	1.13	0.80	1.89	3.82

8.0 Figures

a) Field Site Map

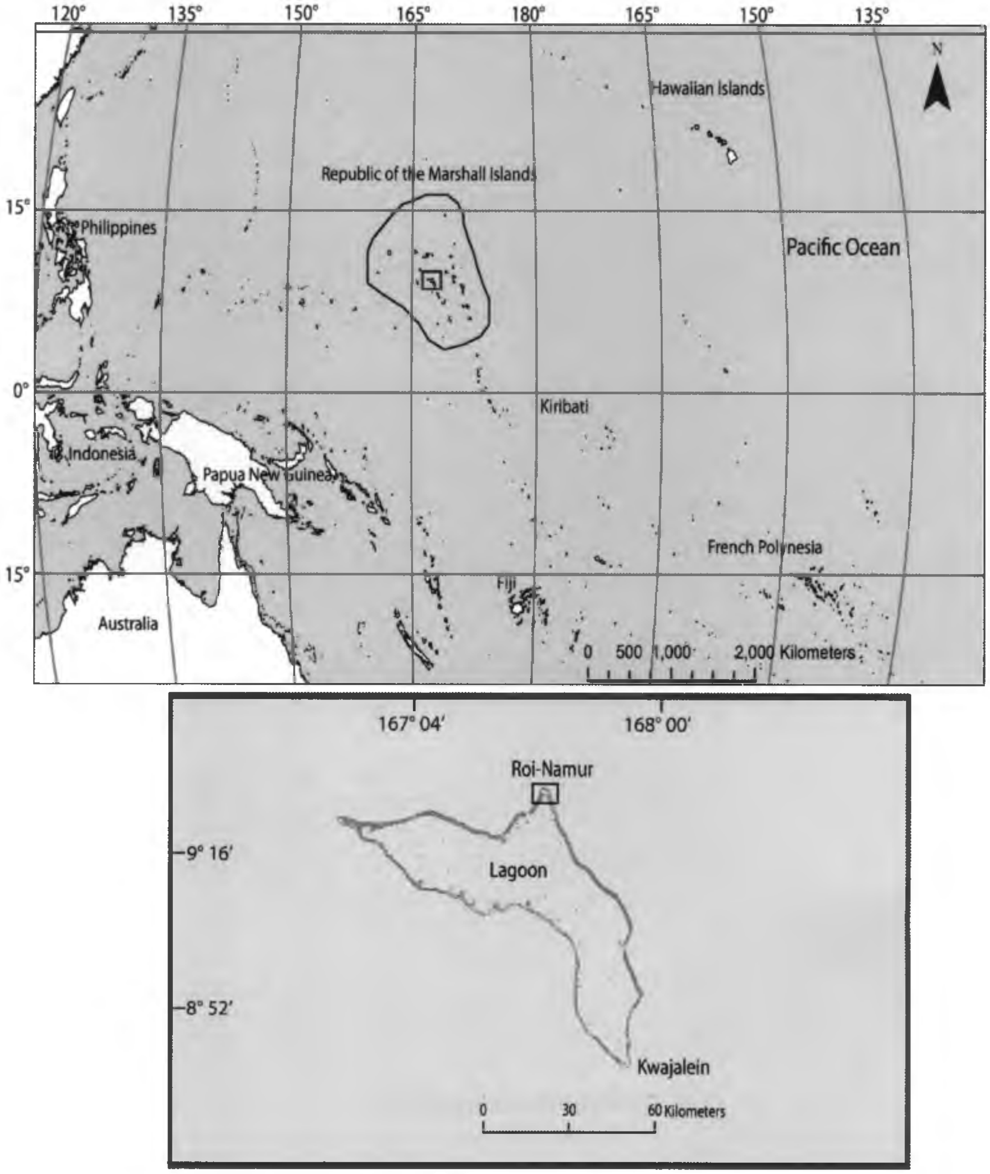

b) Bird’s-Eye View of Roi-Namur

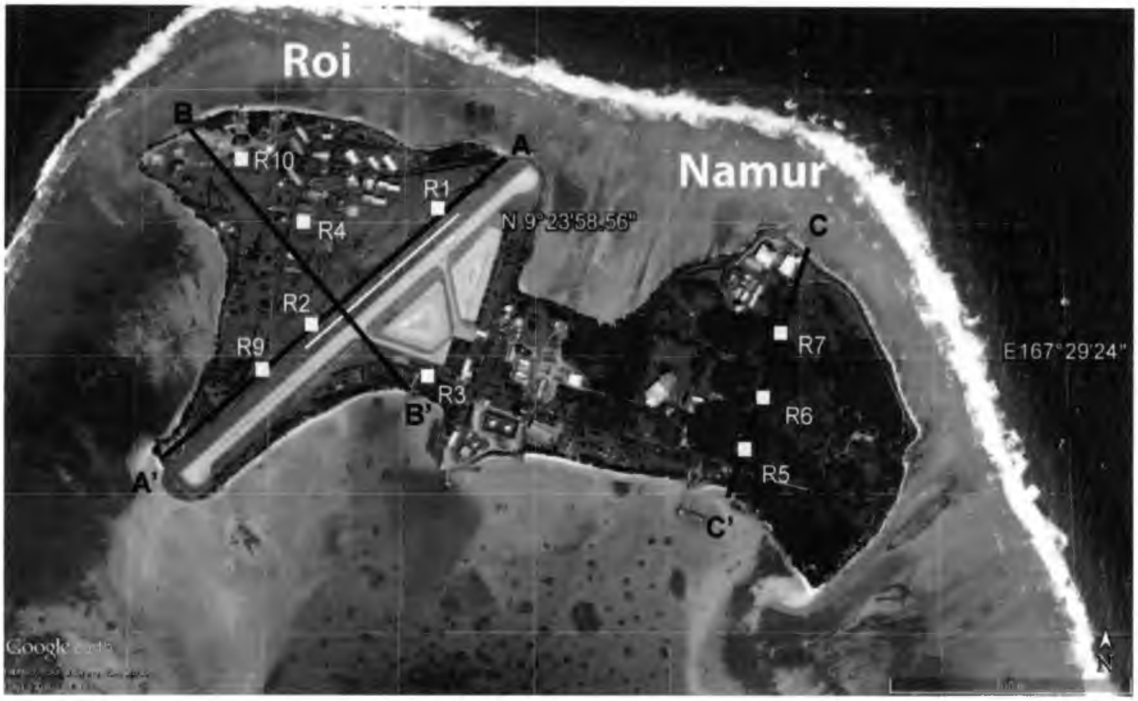

Figure 1. (a) Roi-Namur Island is located on the northern most point of Kwajalein Atoll, Republic of the Marshall Islands. (b) Google Earth image of Roi-Namur shows stark contrast of each lobes landscape. Roi, the western lobe is mostly void of vegetation and contains a 1347-m long runway and two concrete-lined rainwater catchments used to collect rainfall for water supply. Namur is the eastern lobe of the island and has a more typical atoll island setting with thick, jungle-like vegetation. Sampled monitoring wells and ocean to lagoon cross-sections are mapped. White line indicates location of horizontal lens well on Roi.

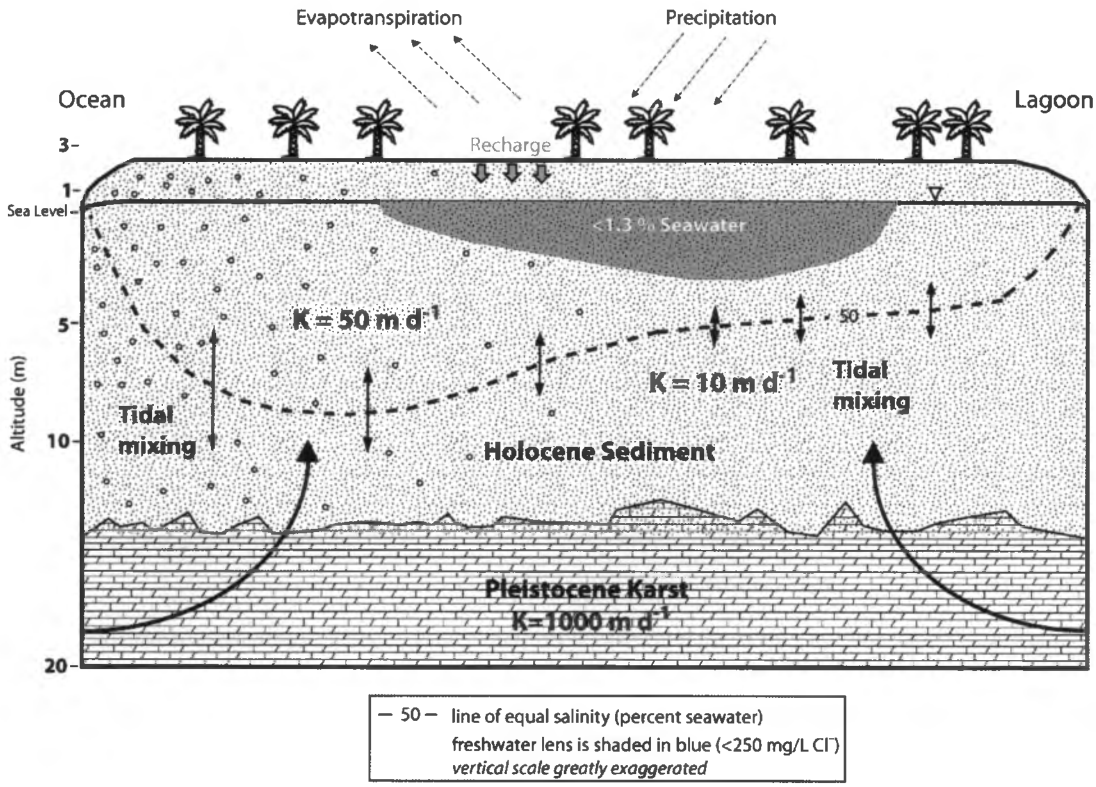

Figure 2. Generalized dual-aquifer conceptual model depicts hydrogeology and tidal mixing in a typical atoll aquifer. Precipitation minus evapotranspiration equals recharge to the FWL. The Pleistocene Karst lies unconformably underneath the Holocene sand and has a hydraulic conductivity that is two to three orders of magnitude greater than the younger deposits. There is a decreasing hydraulic conductivity (K) gradient towards the lower-energy lagoon side of an atoll; a relatively more dampened tidal signal allows for a thicker FWL to develop on the lagoon side of an atoll. In contrast, the FWL on the ocean side is truncated at shallower depths due to greater tidal efficiency and increased tidal mixing.

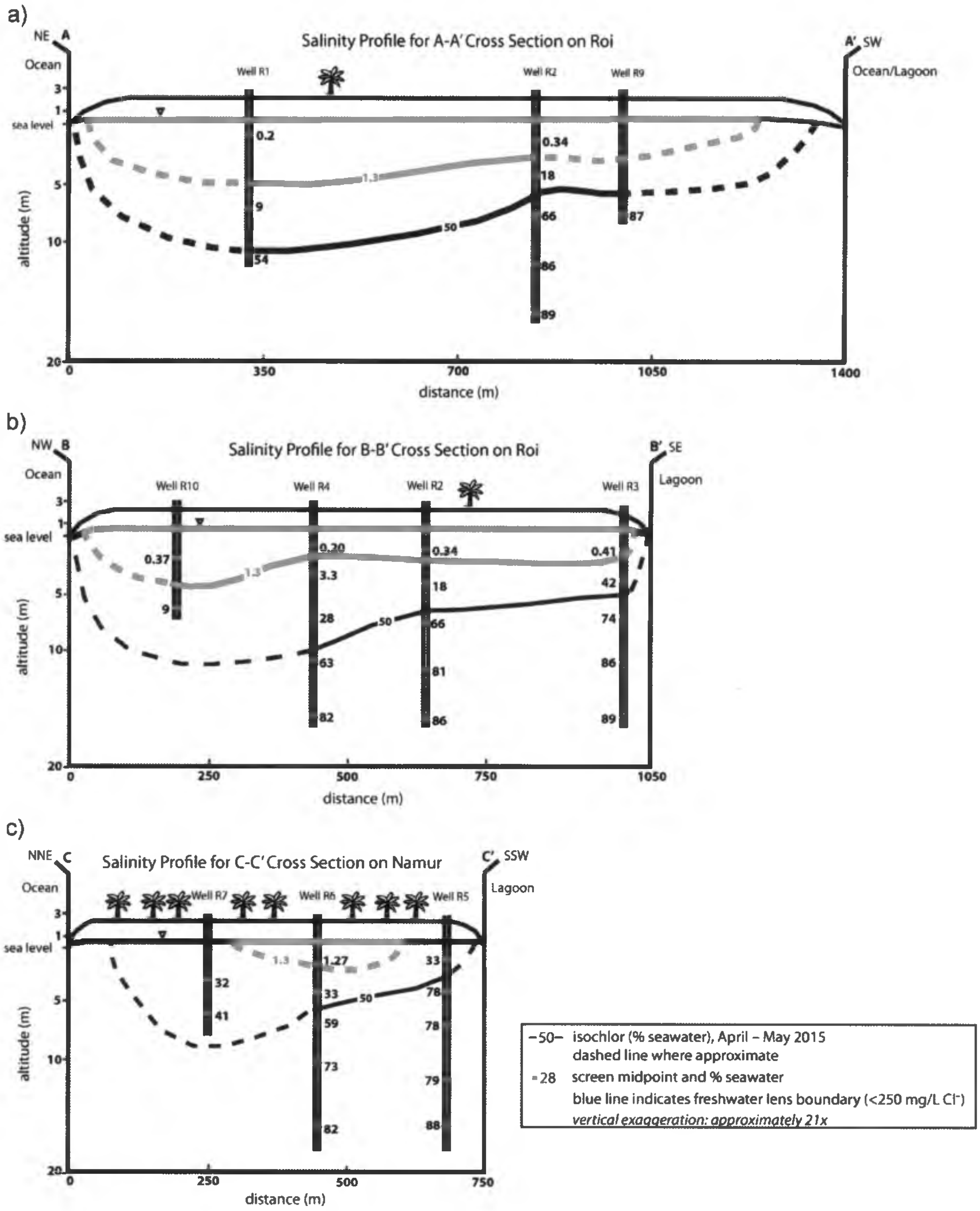

Figure 3. (a–b) Cross sections on Roi indicate a larger FWL overall and a thicker FWL on the ocean side. In contrast, the cross section on (c) Namur indicates a smaller FWL in general and a thicker FWL on the lagoon side, similar to what would be expected with a more natural atoll aquifer.

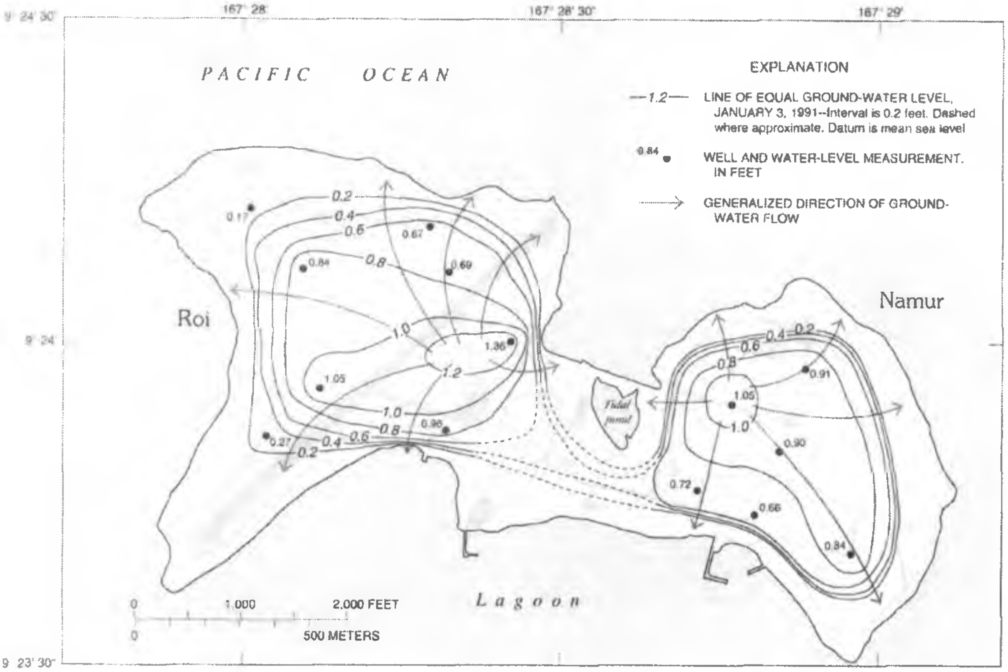

Figure 4. Groundwater levels and predicted flow direction from Gingerich (1996). The map indicates that water recharged west of the runway on Roi will flow towards the ocean side. The hydrogeology on Roi is similar to Namur with respect to location of the highest head and outward radiating flow directions, however, the concrete-lined catchment on Roi has reduced recharge directly underneath the lagoon side.

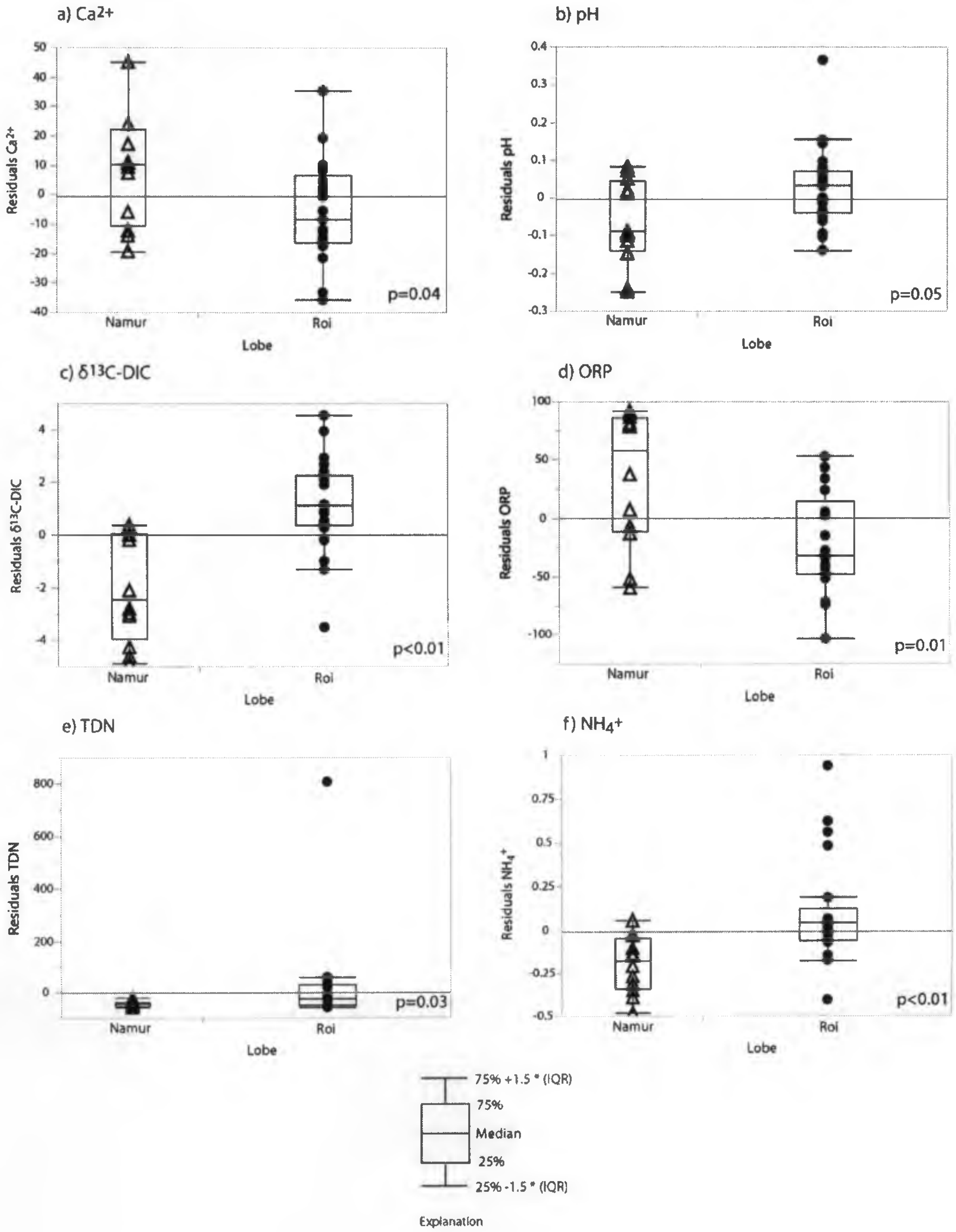

Figure 5. Distributions of residuals for parameters that are significantly different at $\alpha=0.05$. Residuals are calculated from a least squares regression line of combined concentrations from Roi and Namur.

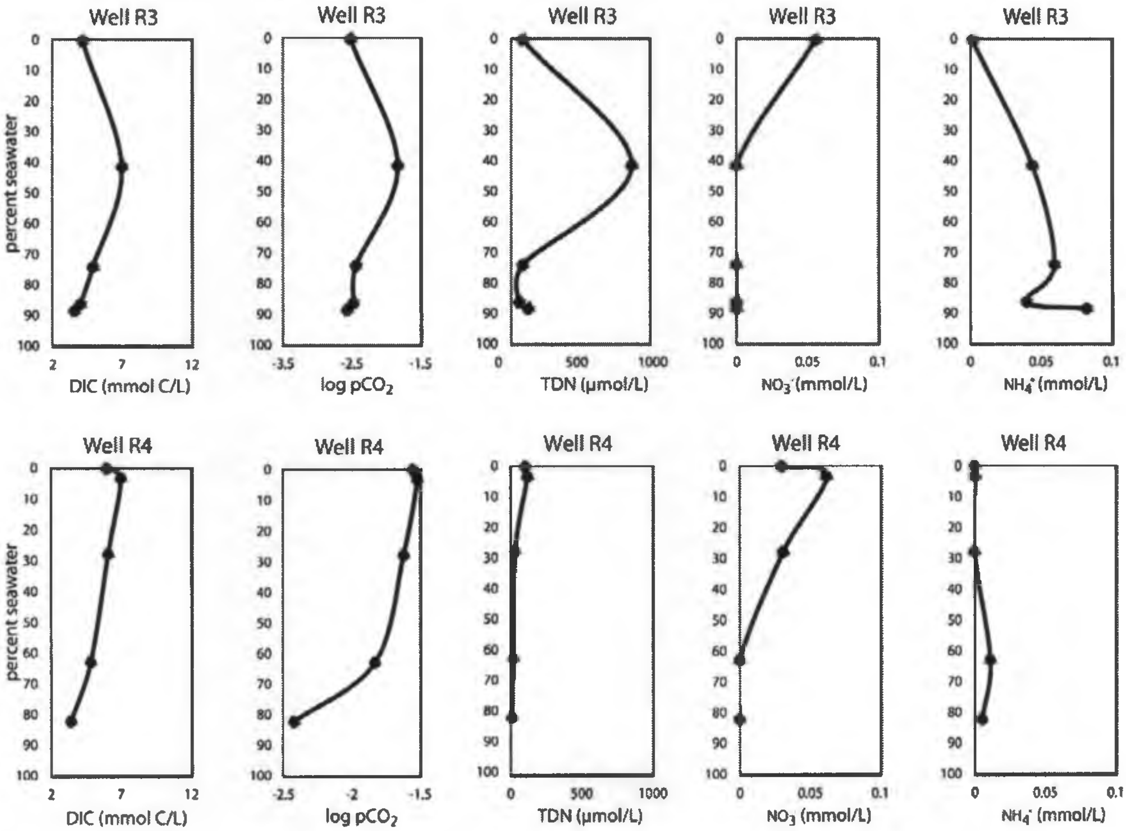

Figure 6. Comparison of elevated DIC, log pCO2, and nutrients at depth for wells R3 and R4. This suggests that point source contamination from septic systems or leaky pipes nearby these well locations are increasing microbial respiration and/or carbonate rock dissolution.

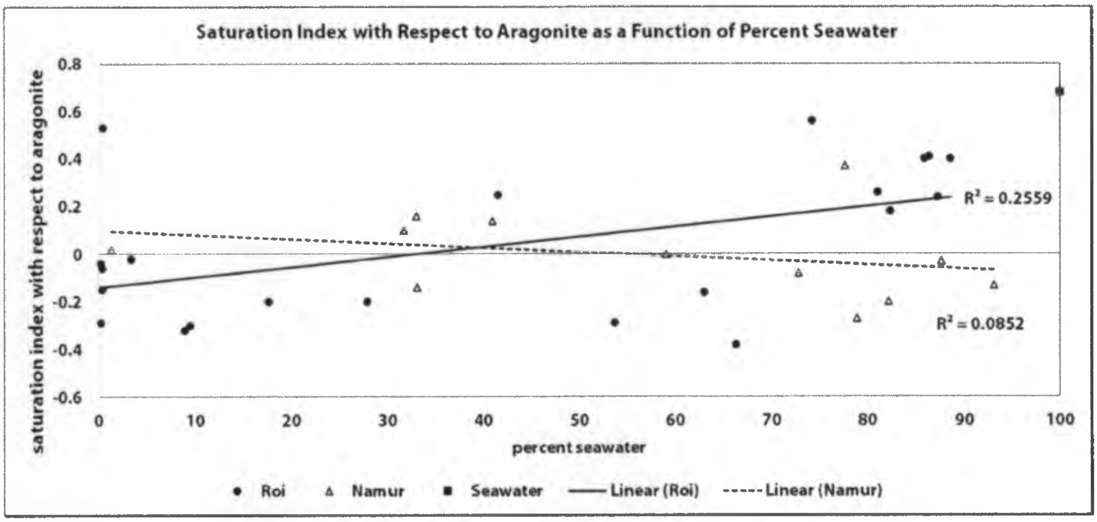

Figure 7. SI on Roi indicates undersaturated conditions in low salinity groundwater (at shallow depths) and supersaturated conditions at higher salinity waters (at deeper depths).

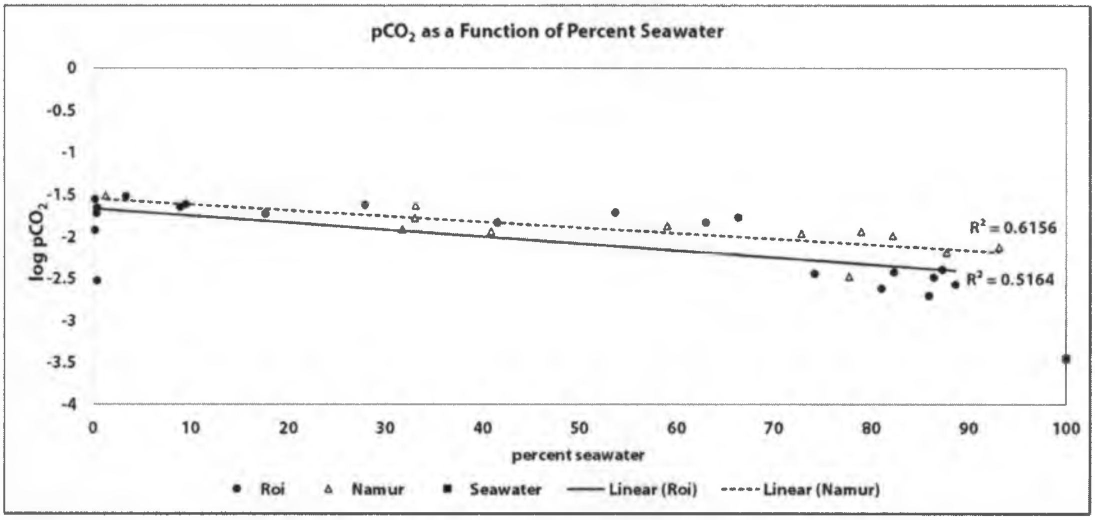

Figure 8. Plot of log pCO2 versus percent seawater. The freshwater lens sample on Namur (<1.3% seawater) has higher pCO2 than the average of the concentrations in the FWL on Roi. Roi also tends to have lower pCO2 concentrations at the most saline waters, indicating CO2 is being transported out of the system quicker than Namur.

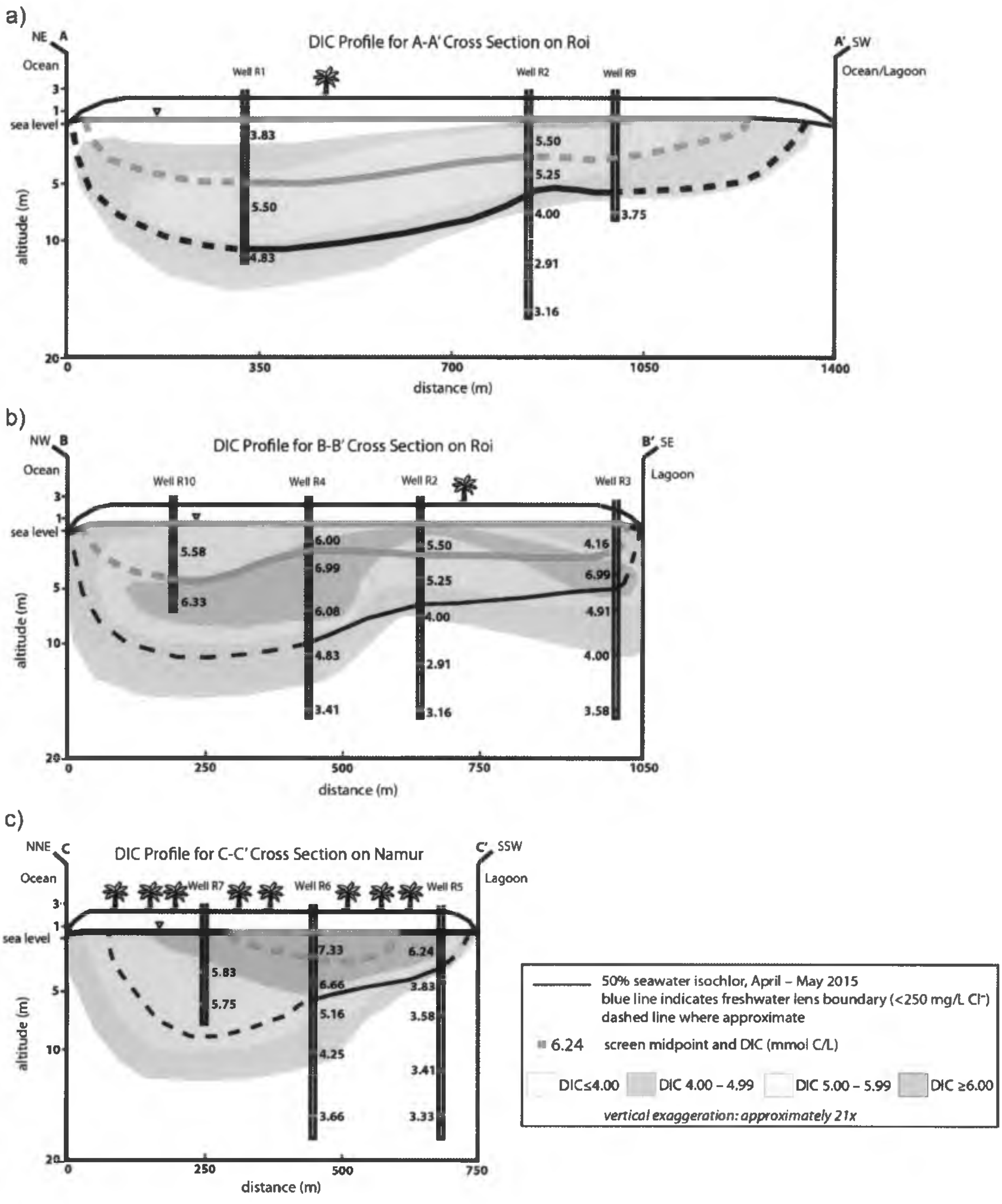

Figure 9. DIC profiles produced from interpolation of sampled groundwater data. Cross sections on (a –b) Roi indicate generally less DIC in the shallow sections of the aquifer compared to (c) Namur. However, there is greater DIC in the intermediate transition zone on Roi than on Namur. Due to LULC change and MAR, enhanced recharge and increased flushing on the ocean side of Roi has shifted geochemical process deeper in the profile.

a) Roi Groundwater Geochemistry Compared to Mixing Model

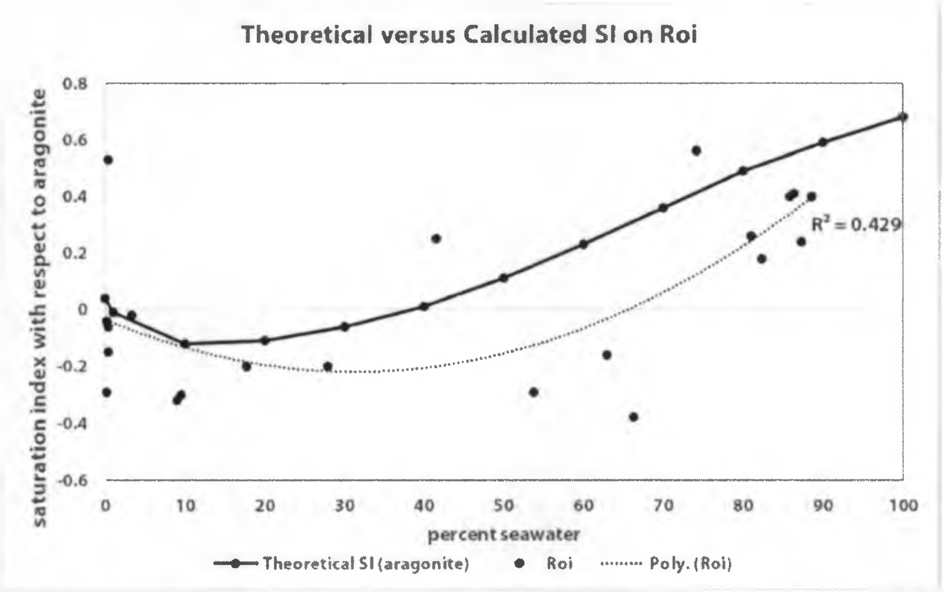

b) Namur Groundwater Geochemistry Compared to Mixing Model

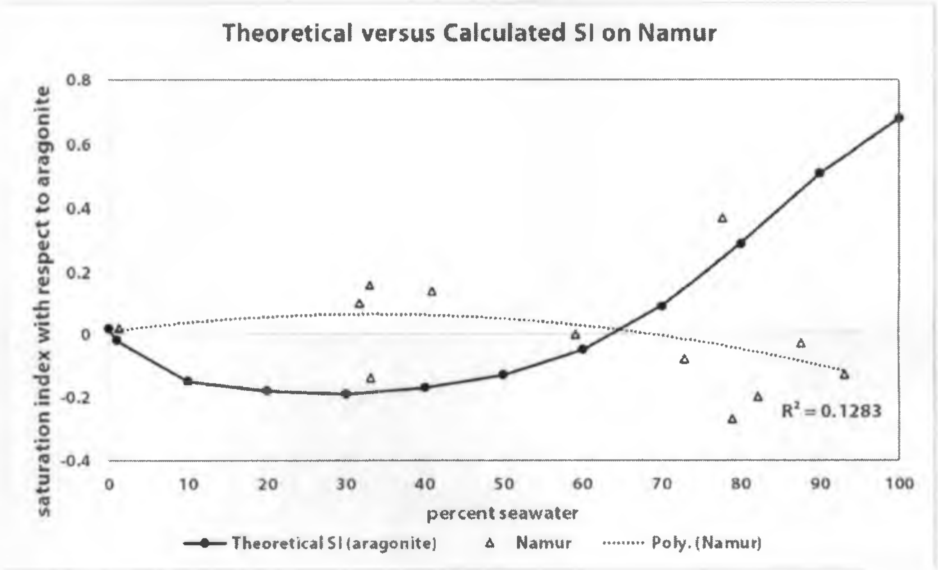

Figure 10. Plot of SI as a function of seawater mix and theoretical mixing scenarios for carbonate groundwater on (a) Roi and (b) Namur. Groundwater chemistry on Roi is more indicative of mixing-dominated processes compared to Namur.

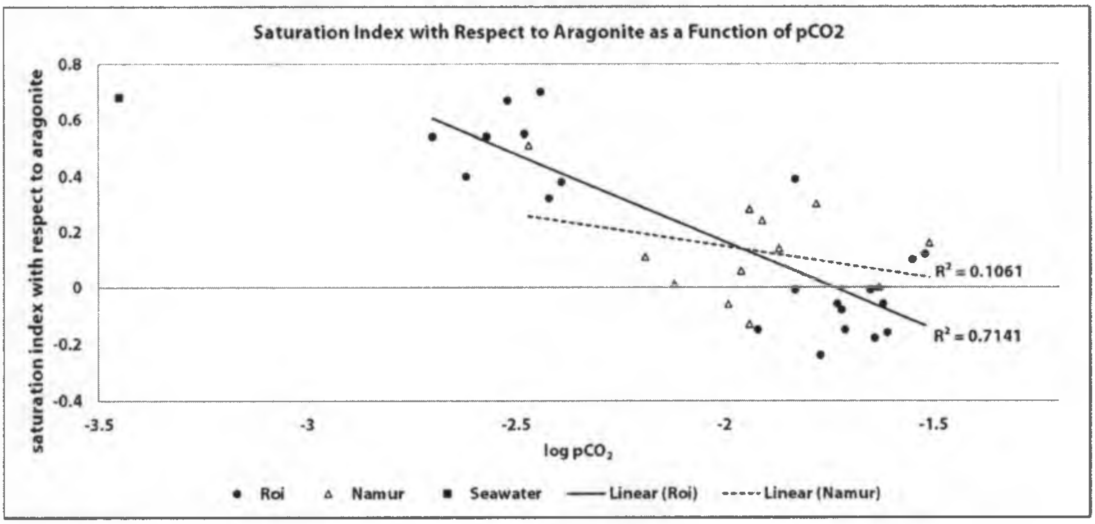

Figure 11. This plot shows a trend of decreasing CO_2 with increasing SI. Groundwater on Roi tends to be more undersaturated or supersaturated and groundwater on Namur is generally closer to saturation.

References

Anthony, S.S., Peterson, F.L., MacKenzie, F.T., Hamlin, S.N., 1989. Geohydrology of the Laura fresh-water lens, Majuro atoll: A hydrogeochemical approach. Geol. Soc. Am. Bull. 101, 1066–1075.

Ayers, J.F., Vacher, H.L., 1986. Hydrogeology of an atoll island: a conceptual model from detailed study of a Micronesian example. Groundwater 24, 185–198.

BADON–GHYBEN, W., 1888. Nota in verband met de voorgenomen putboring nabil Amsterdam'Tijdschr. K. Inst Ing Hague 27, 1888–1889.

Bailey, R.T., Jenson, J.W., Olsen, A.E., 2010. Estimating the Ground Water Resources of Atoll Islands. Water 2, 1–27. doi:10.3390/w2010001

Bailey, R.T., Jenson, J.W., Olsen, A.E., 2009. Numerical Modeling of Atoll Island Hydrogeology. Ground Water 47, 184–196. doi:10.1111/j.1745-6584.2008.00520.x

Bailey, R.T., Jenson, J.W., Rubinstein, D., Olsen, A.E., 2008. Groundwater resources of atoll islands: observations, modeling, and management. Water and Environmental Research Institute of the Western Pacific, University of Guam.

Bailey, R.T., Jenson, J.W., Taboroši, D., 2013. Estimating the freshwater-lens thickness of atoll islands in the Federated States of Micronesia. Hydrogeol. J. 21, 441–457. doi:10.1007/s10040-012-0923-6

Ball, J.W., Nordstrom, D.K., 1991. User's manual for WATEQ4F, with revised thermodynamic data base and test cases for calculating speciation of major, trace, and redox elements in natural waters.

Bonferroni, C.E., 1936. Teoria statistica delle classi e calcolo delle probabilita. Libreria internazionale Seeber.

Buddemeier, R.W., 1981. Geohydrology of Enewetak Atoll islands and reefs. Lawrence Livermore National Lab., CA (USA).

Buddemeier, R.W., Oberdorfer, J.A., 1997. Hydrogeology of Enewetak Atoll, in: Geology and Hydrogeology of Carbonate Islands. Elsevier, pp. 667–692.

Buddemeier, R.W., Oberdorfer, J.A., 1986. Internal Hydrology and Geochemistry of Coral Reefs and Atoll Islands: Key to Diagenetic Variations, in: Schroeder, J.H., Purser, B.H. (Eds.), Reef Diagenesis. Springer Berlin Heidelberg, Berlin, Heidelberg, pp. 91–111.

Dickinson, W.R., 2009. Pacific Atoll Living: How Long Already and Until When? GSA Today 19, 4–10. doi:0.1130/GSATG35A.1

Drever, J.I., 1988. The geochemistry of natural waters, 2nd ed. ed. Prentice Hall, Englewood Cliffs, N.J.

Emery, K.O., Tracey Jr, J.I., Ladd, H.S., 1954. Geology of Bikini and nearby atolls, Marshall Islands.

Falkland, A., 1991. Hydrology and water resources of small islands: a practical guide. UNESCO Press.

Gingerich, S.B., 1996. Ground-water resources and contamination at Roi-Namur Island, Kwajalein Atoll, Republic of the Marshall Islands, 199091 (Water-Resources Investigations Report No. 95–4275). U.S. Geological Survey, Reston, VA.

Gingerich, S.B., 1992. Numerical simulation of the freshwater lens on Roi-Namur island, Kwajalein atoll Repubic of the Marshall Islands. University of Hawaii, Honolulu, Hawaii.

Gurdak, J.J., Allen, D.M., Holding, S., Carvalho Resende, T., Leblanc, M., Aureli, A., Hejazian, M., Swarzenski, P.W., Antoniou, A., Dumont, A., 2015. GRAPHIC Groundwater and climate change: Small Island Developing States (SIDS). United Nations Educational, Scientific, and Cultural Organization (UNESCO)-International Hydrologic Programme (IHP), Paris, France.

Hem, J.D., 1985. Study and interpretation of the chemical characteristics of natural water. Department of the Interior, US Geological Survey.

Herzberg, D., 1901. Die wasserversorgung einiger nordseebäder.

Hunt, C.D., Peterson, F.L., 1980. WRRCTR No. 126 Groundwater Resources of Kwajalein Island, Marshall Islands.

Jevrejeva, S., Moore, J.C., Grinsted, A., 2010. How will sea level respond to changes in natural and anthropogenic forcings by 2100?: SEA LEVEL RESPONSE TO FORCINGS BY 2100. Geophys. Res. Lett. 37, n/a-n/a. doi:10.1029/2010GL042947

Karnauskas, K.B., Donnelly, J.P., Anchukaitis, K.J., 2016. Future freshwater stress for island populations. Nat. Clim. Change. doi:10.1038/nclimate2987

Korom, S.F., 1992. Natural denitrification in the saturated zone: A review. Water Resour. Res. 28, 1657–1668. doi:10.1029/92WR00252

Matthews, R.K., 1971. Diagenetic environments of possible importance to the explanation of cementation fabric in subaerially exposed carbonate sediments. Carbonate Cem. Johns Hopkins Univ. Stud. Geol. 19, 127–132.

Morse, J.W., Mackenzie, F.T., 1990. Geochemistry of sedimentary carbonates. Elsevier.

Oberdorfer, J.A., Hogan, P.J., Buddemeier, R.W., 1990. Atoll island hydrogeology: flow and freshwater occurrence in a tidally dominated system. J. Hydrol. 120, 327–340. doi:10.1016/0022-1694(90)90157-S

Pachauri, R.K., Allen, M.R., Barros, V.R., Broome, J., Cramer, W., Christ, R., Church, J.A., Clarke, L., Dahe, Q., Dasgupta, P., others, 2014. Climate Change 2014: Synthesis Report. Contribution of Working Groups I, II and III to the Fifth Assessment Report of the Intergovernmental Panel on Climate Change.

Parkhurst, D.L., Appelo, C.A.J., 2013. Description of input and examples for PHREEQC version 3: a computer program for speciation, batch-reaction, one-dimensional transport, and inverse geochemical calculations (Report No. 6-A43), Techniques and Methods. Reston, VA.

Plummer, L.N., Vacher, H.L., Mackenzie, F.T., Bricker, O.P., Land, L.S., 1976. Hydrogeochemistry of Bermuda: A case history of ground-water diagenesis of biocalcarenites. Geol. Soc. Am. Bull. 87, 1301. doi:10.1130/0016-7606(1976)87<1301:HOBACH>2.0.CO;2

Raitt, R.W., Perkins, B., 1954. Seismic-refraction studies of Bikini and Kwajalein atolls. US Government Printing Office.

Runnells, D.D., 1969. Diagenesis, Chemical Sediments, and the Mixing of Natural Waters. SEPM J. Sediment. Res. Vol. 39. doi:10.1306/74D71DCA-2B21-11D7-8648000102C1865D

Spennemann, D., 2006. Freshwater lens, settlement patterns, resource use and connectivity in the Marshall Islands. Transform. Cult. EJournal 1.

Thrailkill, J., 1968. Chemical and Hydrologic Factors in the Excavation of Limestone Caves. Geol. Soc. Am. Bull. 79, 19. doi:10.1130/0016-7606(1968)79[19:CAHFIT]2.0.CO;2

Thurber, D.L., Broecker, W.S., Blanchard, R.L., Potratz, H.A., 1965. Uranium-series ages of Pacific atoll coral. Science 149, 55–58.

Tribble, G.W., 1997. Ground-water geochemistry of Kwajalein Island, Republic of the Marshall Islands, 1991. (Water-Resources Investigations Report No. 97–4184). Geological Survey, Honolulu, HI (United States). Water Resources Div., Honolulu, Hawaii.

Underwood, M.R., Peterson, F.L., Voss, C.I., 1992. Groundwatr Lens Dynamics of Atoll Islands. Water Resour. Res. 28, 2889–29902.

U.S. Geological Survey, variously dated. National field manual for the collection of water-quality data (U.S. Geological Survey Techniques of Water-Resources Investigations), book 9, chaps. A1-A9. U.S. Geological Survey, Reston, VA.

Vandenbohede, A., Van Houtte, E., Lebbe, L., 2009. Sustainable groundwater extraction in coastal areas: a Belgian example. Environ. Geol. 57, 735–747.

Voss, C.I., 1984. SUTRA (Saturated-Unsaturated Transport). A Finite-Element Simulation Model for Saturated-Unsaturated, Fluid-Density-Dependent Ground-Water Flow with Energy Transport or Chemically-Reactive Single-Species Solute Transport. DTIC Document.

Wardlaw, B.R., Quinn, T.M., 1991. The record of Pliocene sea-level change at Enewetak Atoll. Quat. Sci. Rev. 10, 247–258. doi:10.1016/0277-3791(91)90023-N

White, I., Falkland, T., Metutera, T., Metai, E., Overmars, M., Perez, P., Dray, A., 2007. Climatic and Human Influences on Groundwater in Low Atolls. Vadose Zone J. 6, 581. doi:10.2136/vzj2006.0092

Wigley, T.M.L., Plummer, L.N., 1976. Mixing of carbonate waters. Geochim. Cosmochim. Acta 40, 989–995. doi:10.1016/0016-7037(76)90041-7

Appendix A

This appendix contains additional laboratory results from groundwater collected on Roi-Namur.

Major and Minor Ion and Trace Element Concentrations

Well or Sample ID	Ba^{2+} (mmol/L)	Br^- (mmol/L)	Cr (mmol/L)	Cs (mmol/L)	Cu (mmol/L)	F (mmol/L)	Fe (mmol/L)	K (mmol/L)
R1-1	4.97E-06	1.38E-03	2.56E-09	ND	2.65E-04	4.17E-03	1.13E-05	0.01
R1-7	2.32E-05	6.87E-02	8.44E-10	2.65E-07	5.93E-07	5.36E-05	2.96E-04	0.99
R1-12	2.82E-05	4.20E-01	2.14E-09	1.21E-06	2.89E-06	1.73E-06	1.09E-04	5.77
R2-1	1.46E-05	2.54E-03	7.64E-10	8.70E-08	1.39E-06	1.14E-03	1.39E-05	0.04
R2-4	3.04E-05	1.39E-01	9.77E-10	6.54E-07	1.59E-07	1.52E-05	1.38E-05	2.00
R2-7	3.73E-05	5.35E-01	1.76E-09	1.53E-06	8.00E-07	1.44E-06	4.48E-05	7.05
R2-12	3.84E-05	6.34E-01	2.49E-09	1.98E-06	5.47E-07	1.05E-06	2.50E-05	8.65
R2-16	3.85E-05	6.82E-01	2.28E-09	1.94E-06	9.34E-07	9.63E-07	2.78E-05	8.36
R3-1	6.17E-06	3.65E-03	5.40E-09	4.11E-08	2.48E-06	2.04E-03	4.34E-05	0.06
R3-4	3.35E-05	3.20E-01	1.73E-09	1.13E-06	3.40E-07	2.76E-06	4.27E-05	4.43
R3-7	4.32E-05	5.96E-01	2.21E-09	2.04E-06	4.17E-07	1.21E-06	1.54E-05	8.01
R3-11	4.87E-05	6.98E-01	2.62E-09	2.02E-06	3.72E-07	9.33E-07	1.50E-05	9.61
R3-16	4.55E-05	6.99E-01	2.61E-09	2.14E-06	7.21E-07	8.09E-07	1.41E-05	10.08
R4-1	8.95E-06	1.66E-03	2.54E-09	2.02E-08	1.13E-05	1.14E-03	2.13E-05	0.02
R4-4	1.35E-05	2.63E-02	1.50E-09	1.88E-07	7.55E-06	1.37E-04	1.04E-05	0.38
R4-7	2.20E-05	2.19E-01	1.23E-09	8.02E-07	1.70E-06	5.81E-06	1.69E-05	3.04
R4-11	3.24E-05	5.00E-01	1.70E-09	1.36E-06	7.07E-07	1.38E-06	3.49E-05	6.71
R4-16	3.94E-05	6.39E-01	1.77E-09	1.76E-06	8.30E-07	9.92E-07	1.05E-04	9.03
R5-1	2.16E-05	2.72E-01	1.90E-09	8.83E-07	3.00E-06	3.16E-06	3.85E-05	3.81
R5-4	3.71E-05	6.30E-01	5.00E-09	1.76E-06	8.05E-07	1.15E-06	2.41E-05	8.59
R5-7	3.82E-05	6.47E-01	1.89E-09	1.85E-06	1.34E-06	1.01E-06	3.14E-05	7.58
R5-12	3.64E-05	6.89E-01	1.84E-09	1.94E-06	7.64E-07	7.85E-07	3.68E-05	9.55
R5-12 d	3.62E-05	6.89E-01	1.85E-09	1.88E-06	6.04E-07	8.04E-07	3.71E-05	9.88
R5-16	3.67E-05	7.54E-01	2.06E-09	1.93E-06	6.88E-07	8.09E-07	7.59E-05	10.26
R6-1	8.56E-06	9.70E-03	1.18E-09	1.03E-07	4.23E-06	7.77E-05	1.08E-05	0.12
R6-4	2.07E-05	2.61E-01	1.21E-09	7.50E-07	4.85E-07	2.81E-06	5.29E-04	3.64
R6-6	2.77E-05	4.68E-01	1.36E-09	1.31E-06	1.08E-06	1.23E-06	2.22E-04	6.31
R6-11	2.98E-05	5.78E-01	1.52E-09	1.59E-06	3.43E-07	9.61E-07	6.68E-04	7.98
R6-16	3.30E-05	6.51E-01	1.55E-09	1.78E-06	1.48E-06	8.96E-07	2.10E-03	9.12
R7-3	1.76E-05	2.54E-01	1.14E-08	7.17E-07	7.28E-06	3.16E-06	1.97E-05	3.44
R7-6	1.88E-05	3.26E-01	1.30E-08	9.19E-07	5.69E-06	2.29E-06	1.39E-05	4.59
R9-8	4.18E-05	6.96E-01	2.43E-09	1.82E-06	7.49E-07	8.18E-07	1.96E-05	9.60
R9-8 d	4.23E-05	6.97E-01	2.37E-09	1.82E-06	5.71E-07	7.94E-07	2.39E-05	9.35
R10-2	8.06E-06	2.85E-03	2.72E-09	4.50E-08	1.94E-04	2.57E-03	9.20E-06	0.04
R10-6	1.55E-05	7.31E-02	7.89E-10	3.06E-07	1.60E-06	5.21E-05	2.06E-04	1.05
seawater	3.19E-05	7.90E-01	4.75E-09	2.12E-06	1.06E-05	6.35E-07	1.92E-05	10.85
seawater d	3.09E-05	7.69E-01	4.44E-09	2.10E-06	5.20E-06	7.56E-07	2.12E-05	10.00
rain	1.55	ND	-	-	3.23E-08	ND	3.87E-09	ND
catchment	ND	2.15E-04	2.32E-09	1.16E-08	1.77E-05	7.28E-04	4.89E-05	ND
field blank	ND	ND	ND	1.70E-08	1.08E-05	2.03E-04	8.58E-05	ND

Major and Minor Ion and Trace Element Concentrations

Well or Sample ID	Mn (mmol/L)	Na (mmol/L)	Ni (mmol/L)	P (mmol/L)	Pb (mmol/L)	Re (mmol/L)	Si (mmol/L)	U (mmol/L)	V (mmol/L)
R1-1	1.55E-05	1.16	4.09E-06	1.23E-04	7.16E-08	1.33E-13	5.40E-03	8.96E-07	2.84E-08
R1-7	2.59E-05	44.79	5.24E-06	2.21E-04	8.08E-08	3.23E-12	1.63E-03	2.09E-06	1.29E-09
R1-12	2.49E-05	229.60	5.17E-06	2.83E-04	1.75E-07	8.67E-12	2.82E-03	5.15E-07	2.67E-09
R2-1	1.21E-05	2.06	6.92E-06	1.15E-04	4.40E-08	4.05E-13	4.06E-03	2.16E-06	2.84E-08
R2-4	1.20E-05	90.10	1.49E-05	2.61E-05	5.91E-08	1.50E-12	3.97E-03	1.08E-07	6.73E-10
R2-7	1.36E-05	284.01	5.60E-06	2.45E-04	9.50E-08	5.98E-13	2.75E-03	2.73E-07	1.57E-09
R2-12	2.16E-05	349.94	3.51E-06	2.22E-04	7.82E-08	5.97E-13	2.01E-03	2.89E-07	1.25E-09
R2-16	1.41E-05	392.20	2.93E-06	2.82E-04	8.94E-08	1.08E-12	3.62E-03	3.47E-07	4.31E-10
R3-1	8.94E-06	2.40	4.40E-06	1.03E-04	4.89E-08	4.89E-13	1.39E-02	9.43E-07	1.95E-08
R3-4	7.34E-06	216.47	9.55E-06	3.09E-04	1.09E-07	1.49E-12	6.09E-03	3.47E-07	1.34E-09
R3-7	2.16E-05	328.58	5.41E-06	4.41E-04	5.78E-08	2.59E-12	3.17E-03	1.86E-07	1.43E-09
R3-11	2.85E-05	399.11	4.78E-06	4.06E-04	9.14E-08	2.46E-12	1.55E-03	3.04E-06	3.96E-09
R3-16	1.35E-05	420.84	4.45E-06	3.51E-04	9.63E-08	2.17E-12	4.27E-03	5.85E-07	2.04E-09
R4-1	8.22E-06	1.39	1.91E-05	8.76E-05	1.07E-07	4.46E-13	2.13E-02	1.24E-06	3.74E-08
R4-4	6.82E-06	18.15	1.39E-05	1.27E-04	8.93E-08	1.11E-12	2.74E-02	3.01E-06	4.04E-08
R4-7	2.83E-05	141.48	2.51E-05	1.16E-04	1.27E-07	4.78E-12	8.71E-03	1.41E-05	1.76E-07
R4-11	1.08E-05	265.89	4.87E-06	2.26E-04	1.27E-07	1.15E-12	2.22E-03	2.38E-07	9.07E-10
R4-16	2.48E-05	372.69	2.67E-06	2.52E-04	7.77E-08	3.04E-12	1.42E-03	4.68E-07	1.02E-09
R5-1	2.41E-05	176.89	1.25E-05	8.07E-05	1.15E-07	1.04E-12	1.38E-02	1.19E-06	4.75E-09
R5-4	1.46E-05	349.32	3.36E-06	2.65E-04	1.16E-07	1.00E-12	7.16E-03	5.73E-07	4.77E-08
R5-7	1.04E-05	345.49	4.25E-06	2.76E-04	1.79E-07	9.08E-13	7.65E-03	4.91E-07	1.34E-09
R5-12	1.93E-05	406.88	2.36E-06	2.80E-04	7.93E-08	1.52E-12	4.51E-03	3.42E-07	1.09E-09
R5-12 d	1.95E-05	439.52	2.15E-06	2.63E-04	7.78E-08	1.74E-12	4.58E-03	3.35E-07	1.57E-11
R5-16	2.12E-05	432.55	3.24E-06	2.74E-04	8.88E-08	2.75E-12	4.23E-03	7.32E-07	8.04E-10
R6-1	4.36E-07	7.93	7.46E-06	1.24E-04	7.20E-08	3.11E-13	1.79E-02	1.45E-06	1.34E-08
R6-4	4.82E-05	169.80	2.18E-05	2.18E-04	8.34E-08	1.69E-12	9.18E-03	2.58E-07	1.11E-09
R6-6	8.87E-05	251.57	2.87E-05	1.30E-04	1.03E-07	2.41E-12	3.80E-03	7.67E-07	6.92E-10
R6-11	9.30E-05	322.56	1.62E-05	3.21E-04	6.98E-08	2.87E-12	8.60E-03	1.01E-06	5.60E-10
R6-16	6.37E-05	371.33	9.15E-06	1.72E-04	6.94E-08	2.78E-12	4.99E-03	1.20E-06	4.03E-10
R7-3	5.59E-06	155.38	6.19E-06	1.73E-04	1.23E-07	1.89E-12	2.31E-03	4.94E-06	2.32E-08
R7-6	ND	210.82	7.06E-06	2.55E-04	9.95E-08	2.09E-12	4.39E-03	5.32E-06	2.36E-08
R9-8	1.47E-05	408.54	4.46E-06	5.53E-04	7.84E-08	1.25E-12	1.87E-03	2.76E-07	9.92E-10
R9-8 d	1.55E-05	399.18	4.16E-06	5.56E-04	1.01E-07	1.69E-12	1.82E-03	2.88E-07	1.64E-09
R10-2	6.09E-06	2.31	1.17E-05	1.14E-04	4.49E-08	1.94E-13	1.71E-02	1.43E-06	2.61E-08
R10-6	6.83E-06	48.10	8.31E-06	1.34E-04	1.52E-07	8.45E-13	1.47E-02	4.20E-07	4.57E-10
seawater	ND	458.24	2.62E-06	1.87E-04	8.14E-08	4.86E-12	4.36E-04	1.04E-05	3.25E-08
seawater d	ND	473.20	2.91E-06	2.12E-04	9.67E-08	3.81E-12	4.54E-04	1.03E-05	2.99E-08
rain	5.38E-10	0.07	3.89E-09	-	3.74E-10	-	-	1.21E-12	-
catchment	1.75E-05	0.25	2.69E-06	2.84E-05	2.54E-07	9.88E-14	3.04E-03	5.96E-08	4.62E-09
field blank	5.28E-06	ND	6.13E-07	1.98E-05	1.86E-07	1.91E-13	1.74E-04	ND	ND

Appendix B

This appendix lists the source rock contributions from each well.

Excess Ions in Solution from Carbonate Rock Dissolution

well or sample ID	measured Ca^{2+} (mmol/L)	Ca^{2+} derived from source rock	measured Mg^{2+} (mmol/L)	Mg^{2+} derived from source rock	measured HCO_3^- (mmol/L)	HCO_3^- derived from source rock
R1-1	1.14	1.12	0.89	0.78	3.46	3.46
R1-7	2.47	1.53	5.89	0.91	4.82	4.61
R1-12	6.92	1.32	30.88	0.96	4.32	3.11
R2-1	1.74	1.70	1.22	1.03	4.92	4.91
R2-4	3.79	1.94	10.19	0.34	3.18	2.78
R2-7	8.29	1.37	37.34	0.39	3.56	2.06
R2-12	9.26	0.80	43.96	-1.18	2.95	1.12
R2-16	9.65	0.68	47.94	0.09	3.25	1.31
R3-1	1.52	1.48	0.78	0.55	-	-
R3-4	6.80	2.46	26.33	3.17	6.68	5.74
R3-7	9.19	1.45	43.10	1.76	5.00	3.33
R3-11	9.92	0.90	49.60	1.45	4.05	2.10
R3-16	10.32	1.07	51.50	2.13	3.65	1.65
R4-1	2.28	2.26	0.62	0.51	5.15	5.15
R4-4	2.81	2.46	2.50	0.63	6.11	6.04
R4-7	4.88	1.96	16.22	0.67	5.40	4.77
R4-11	7.56	0.98	35.35	0.25	4.45	3.03
R4-16	9.45	0.86	47.24	1.35	-	-
R5-1	5.72	2.27	20.23	1.79	5.61	4.86
R5-4	9.50	1.38	44.33	1.04	-	-
R5-7	8.95	0.71	42.59	-1.40	3.31	1.53
R5-12	10.10	0.95	50.58	1.74	3.30	1.32
R5-12 d	10.85	-	54.40	-	-	-
R5-16	10.41	0.69	53.31	1.43	3.18	1.08
R6-1	2.41	2.28	1.87	1.16	6.40	6.37
R6-4	6.25	2.80	19.02	0.61	6.24	5.50
R6-6	7.99	1.83	33.23	0.33	4.84	3.51
R6-11	9.13	1.52	41.75	1.16	3.99	2.35
R6-16	9.43	0.85	47.08	1.27	3.43	1.58
R7-3	5.23	1.92	17.64	-0.04	-	-
R7-6	6.46	2.19	23.74	0.92	-	-
R9-8	10.21	1.09	51.33	2.71	3.73	1.76
R9-8 d	10.13	0.96	50.48	1.55	3.73	1.75
R10-2	1.62	1.58	1.31	1.10	4.89	4.88
R10-6	2.08	1.09	6.78	1.50	5.60	5.39
seawater	10.44	-	55.73	-	2.26	-
seawater d	10.65	-	54.31	-	-	-

Appendix C

This appendix shows the plots of groundwater quality versus percent seawater for parameters selected for statistical analysis on Roi-Namur.

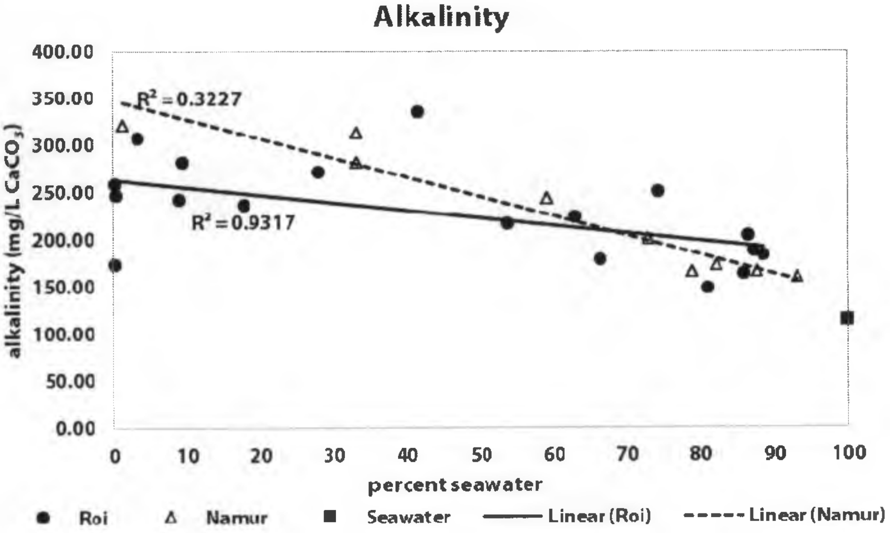

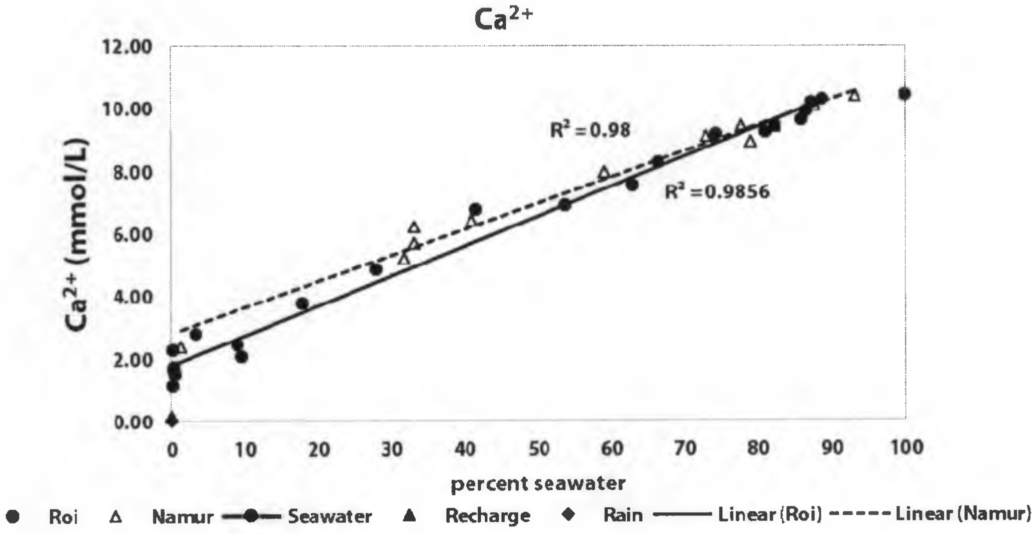
Ca2+
12.00
10.00
8.00
6.00
4.00
2.00
0.00
Ca2+ (mmol/L)
R² = 0.98
R² = 0.9856
0
10
20
30
40
50
60
70
80
90
100
percent seawater
● Roi
△ Namur
—●— Seawater
▲ Recharge
◆ Rain
—— Linear (Roi)
----- Linear (Namur)

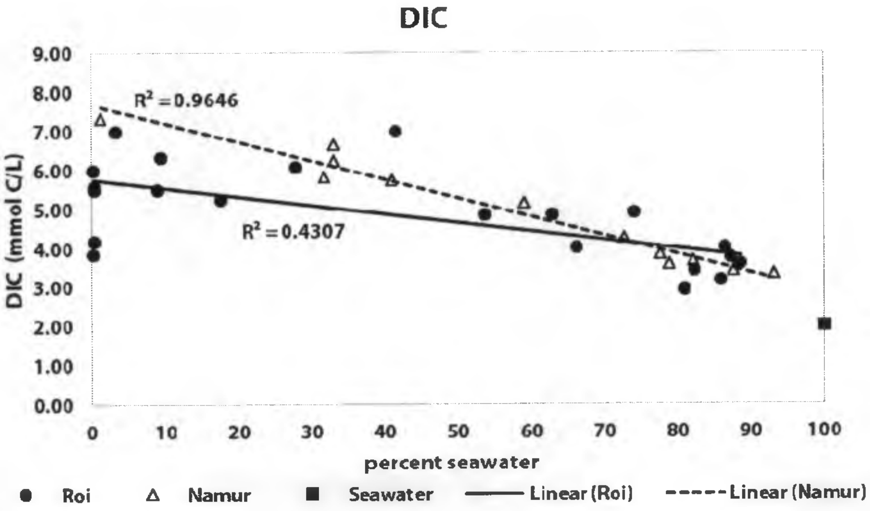
DIC
9.00
8.00
7.00
6.00
5.00
4.00
3.00
2.00
1.00
0.00
DIC (mmol C/L)
R² = 0.9646
R² = 0.4307
0
10
20
30
40
50
60
70
80
90
100
percent seawater
● Roi
△ Namur
■ Seawater
—— Linear (Roi)
----- Linear (Namur)

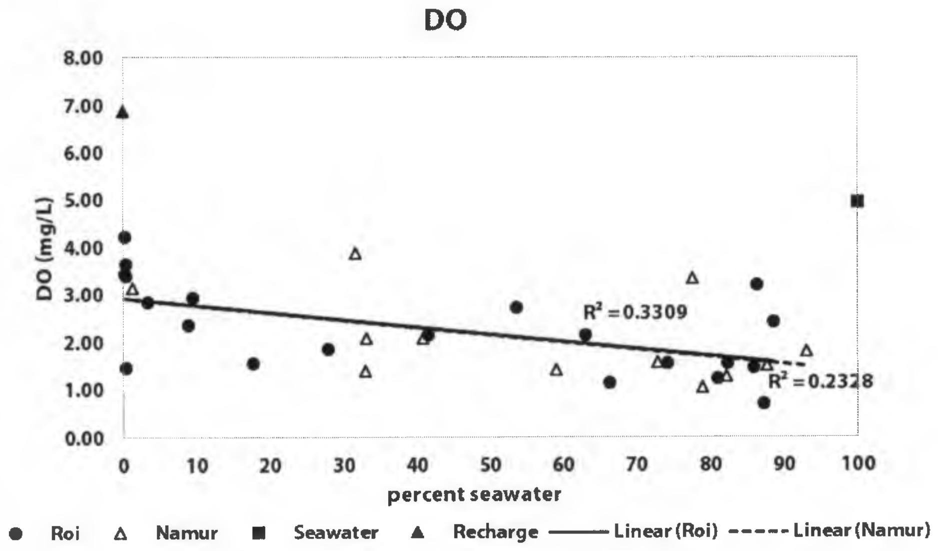
DO
DO (mg/L)
8.00
7.00
6.00
5.00
4.00
3.00
2.00
1.00
0.00
0
10
20
30
40
50
60
70
80
90
100
percent seawater
R² = 0.3309
R² = 0.2328
● Roi
△ Namur
■ Seawater
▲ Recharge
Linear (Roi)
Linear (Namur)

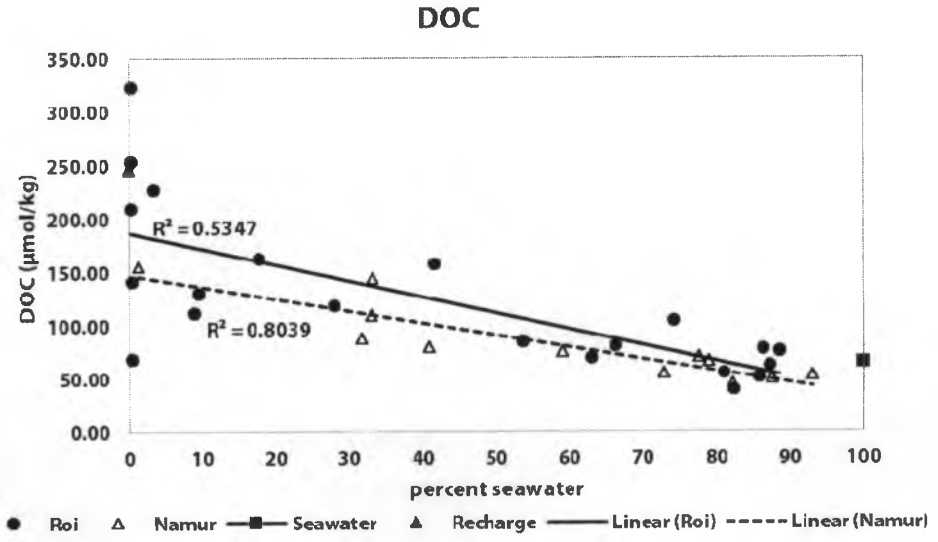
DOC
DOC (µmol/kg)
350.00
300.00
250.00
200.00
150.00
100.00
50.00
0.00
0
10
20
30
40
50
60
70
80
90
100
percent seawater
R² = 0.5347
R² = 0.8039
● Roi
△ Namur
■ Seawater
▲ Recharge
Linear (Roi)
Linear (Namur)

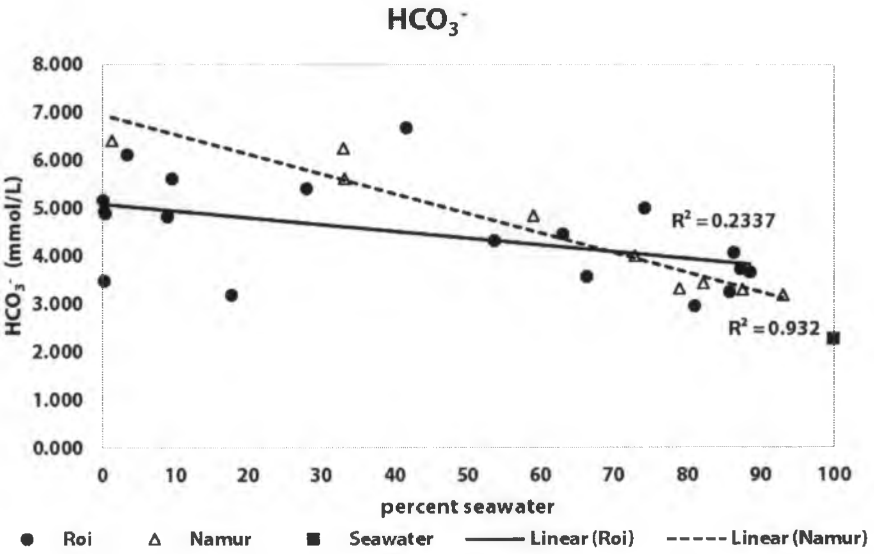
HCO₃⁻
8.000
7.000
6.000
5.000
4.000
3.000
2.000
1.000
0.000
HCO₃⁻ (mmol/L)
0
10
20
30
40
50
60
70
80
90
100
percent seawater
R² = 0.2337
R² = 0.932
● Roi
△ Namur
■ Seawater
—— Linear (Roi)
----- Linear (Namur)

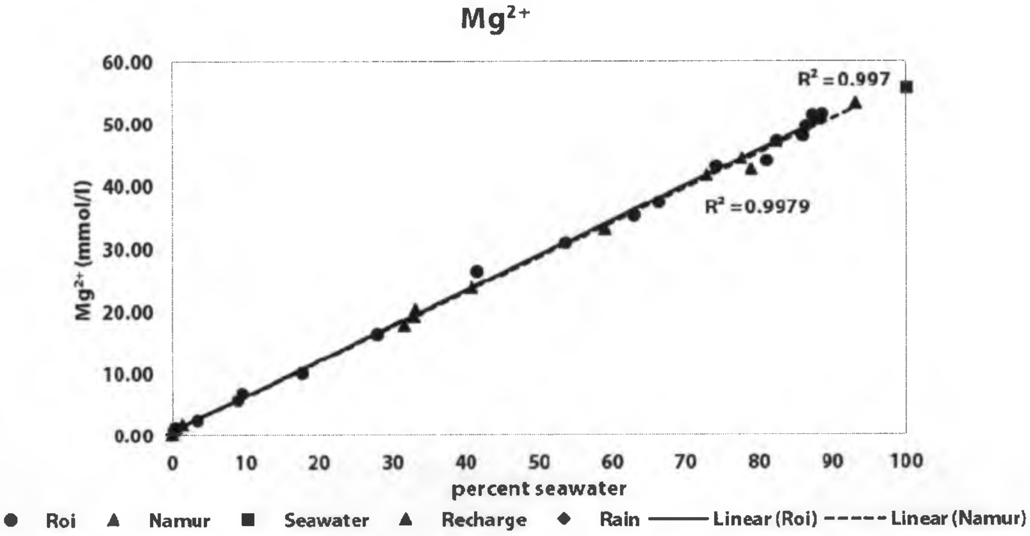
Mg²⁺
60.00
50.00
40.00
30.00
20.00
10.00
0.00
Mg²⁺ (mmol/l)
0
10
20
30
40
50
60
70
80
90
100
percent seawater
R² = 0.997
R² = 0.9979
● Roi
▲ Namur
■ Seawater
▲ Recharge
◆ Rain
—— Linear (Roi)
----- Linear (Namur)

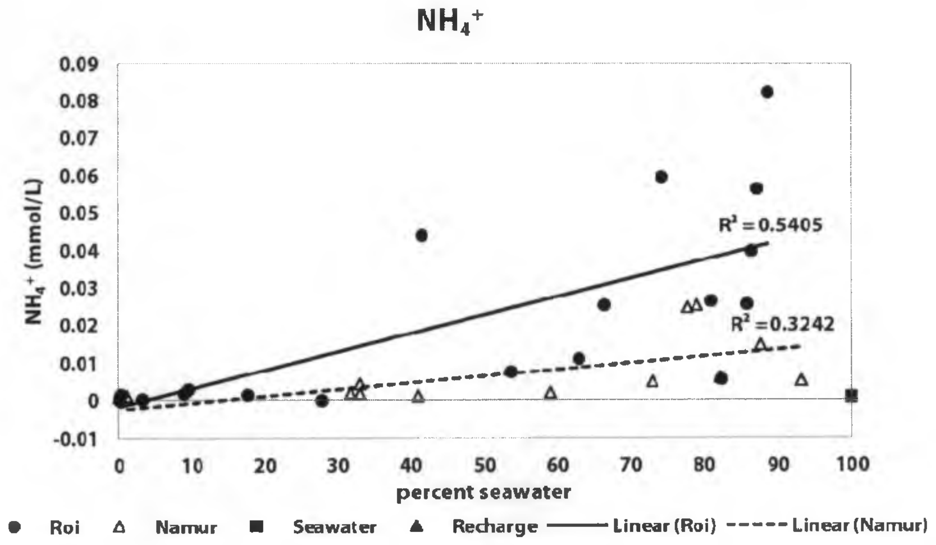
NH₄⁺
NH₄⁺ (mmol/L)
0.09
0.08
0.07
0.06
0.05
0.04
0.03
0.02
0.01
0
-0.01
0
10
20
30
40
50
60
70
80
90
100
percent seawater
R² = 0.5405
R² = 0.3242
● Roi
△ Namur
■ Seawater
▲ Recharge
Linear (Roi)
Linear (Namur)

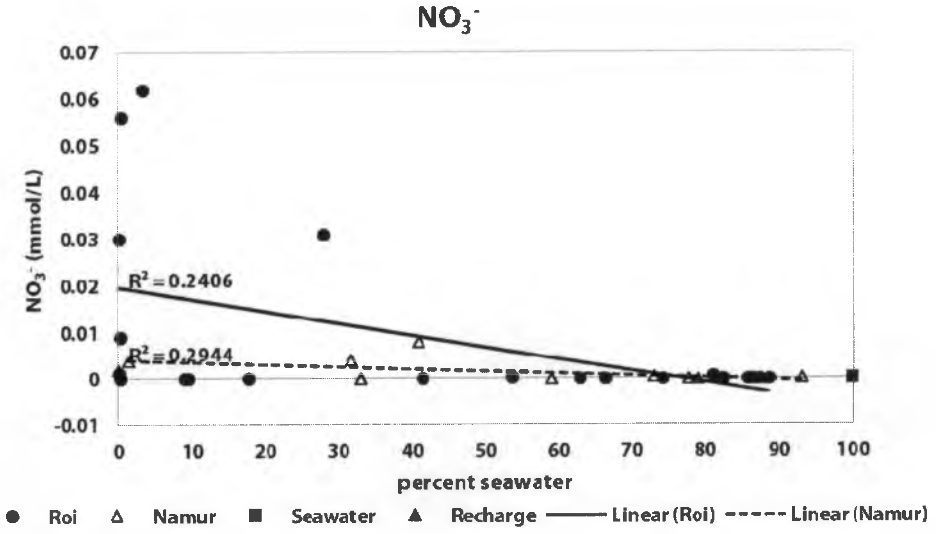
NO₃⁻
NO₃⁻ (mmol/L)
0.07
0.06
0.05
0.04
0.03
0.02
0.01
0
-0.01
0
10
20
30
40
50
60
70
80
90
100
percent seawater
R² = 0.2406
R² = 0.2944
● Roi
△ Namur
■ Seawater
▲ Recharge
Linear (Roi)
Linear (Namur)

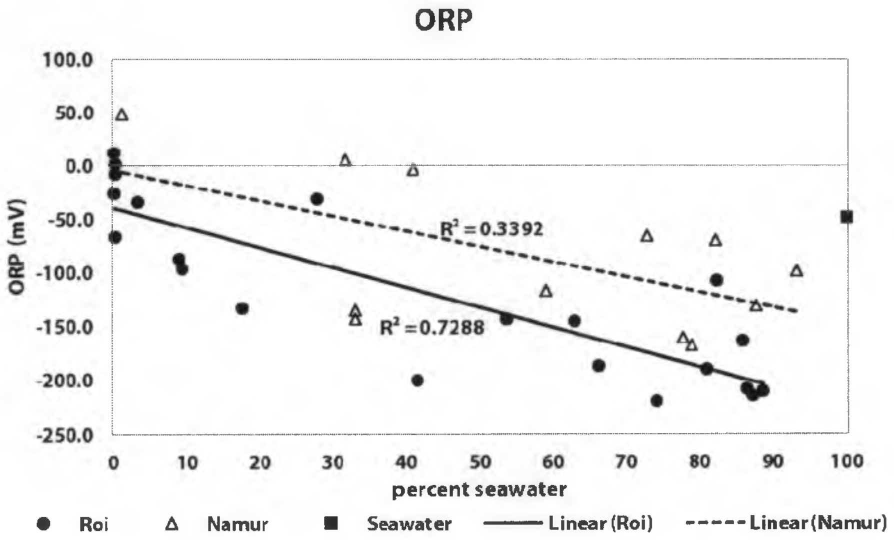
ORP
100.0
50.0
0.0
-50.0
-100.0
-150.0
-200.0
-250.0
ORP (mV)
0
10
20
30
40
50
60
70
80
90
100
percent seawater
R² = 0.3392
R² = 0.7288
● Roi
Δ Namur
■ Seawater
Linear (Roi)
Linear (Namur)

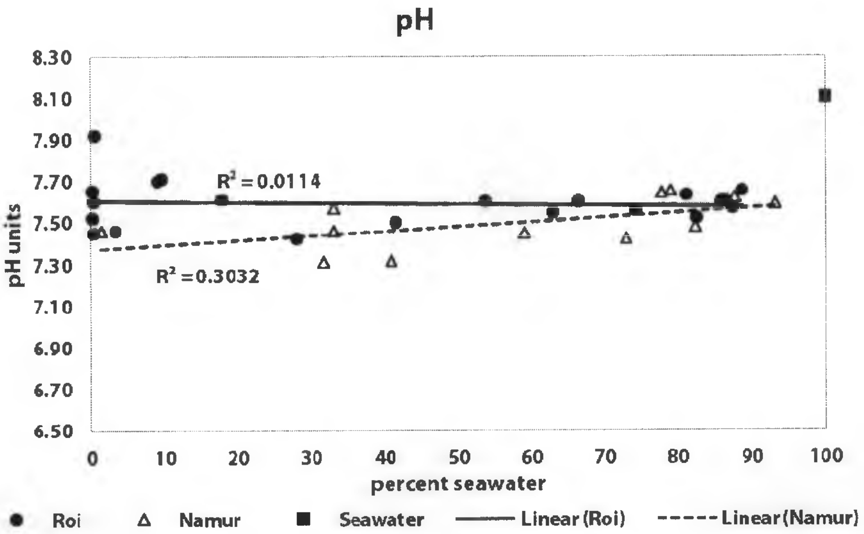
pH
8.30
8.10
7.90
7.70
7.50
7.30
7.10
6.90
6.70
6.50
pH units
0
10
20
30
40
50
60
70
80
90
100
percent seawater
R² = 0.0114
R² = 0.3032
● Roi
Δ Namur
■ Seawater
Linear (Roi)
Linear (Namur)

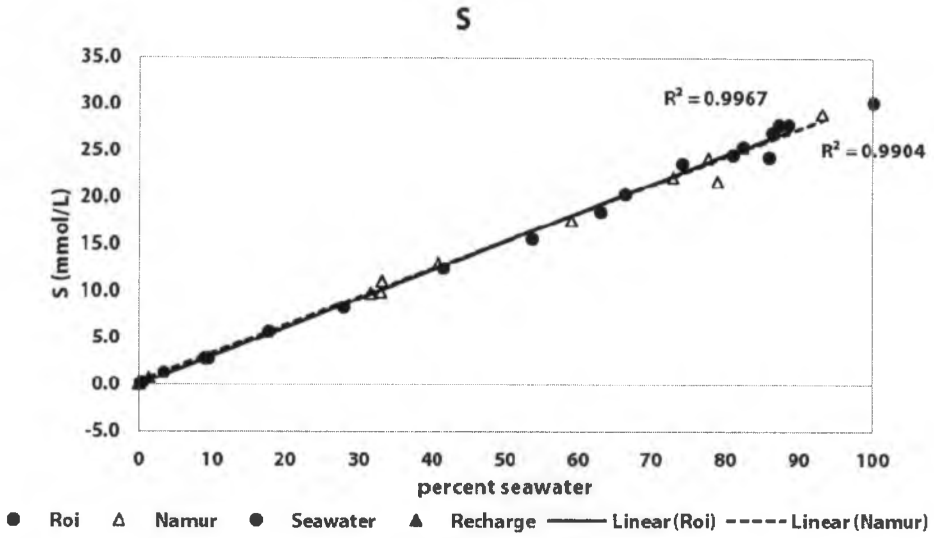
S

35.0
30.0
25.0
20.0
15.0
10.0
5.0
0.0
-5.0
S (mmol/L)
R² = 0.9967
R² = 0.9904
0
10
20
30
40
50
60
70
80
90
100
percent seawater
● Roi
Δ Namur
● Seawater
▲ Recharge
Linear (Roi)
Linear (Namur)

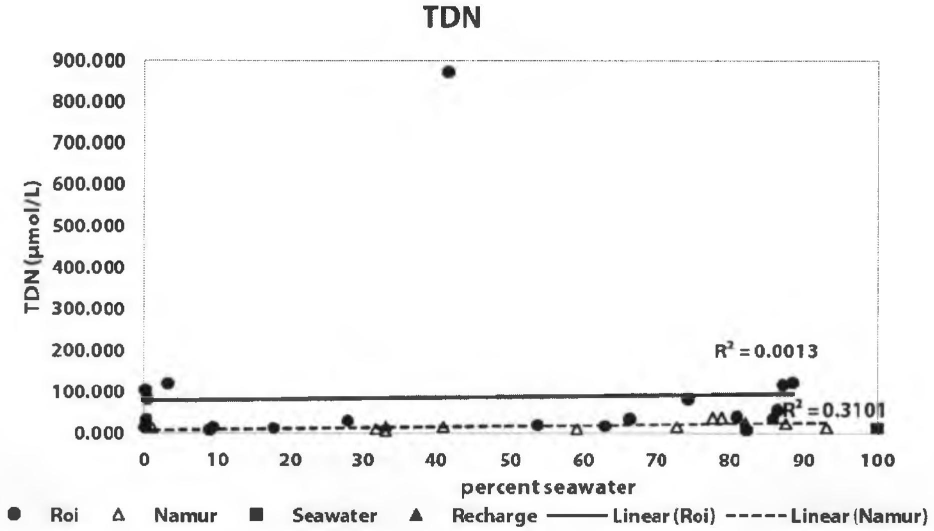
TDN

900.000
800.000
700.000
600.000
500.000
400.000
300.000
200.000
100.000
0.000
TDN (µmol/L)
R² = 0.0013
R² = 0.3101
0
10
20
30
40
50
60
70
80
90
100
percent seawater
● Roi
Δ Namur
■ Seawater
▲ Recharge
Linear (Roi)
Linear (Namur)